Energy and Built Environment xxx (xxxx) xxx

Contents lists available at ScienceDirect

Energy and Built Environment

journal homepage: http://www.keaipublishing.com/en/journals/energy-and-built-environment/

Full Length Article

Parametric analysis of a novel rotary scoop dual-channel windcatcher for multi-directional natural ventilation of buildings

Jiaxiang Li[a,c], John Calautit[a,*], Carlos Jimenez-Bescos[b]

[a] Department of Architecture and Built Environment, University of Nottingham, UK
[b] Westminster Business School, University of Westminster, UK
[c] College of Engineering, Eastern Institute of Technology, Ningbo 315200, China

ARTICLE INFO

Keywords:
Buildings
CFD
Natural ventilation
Windcatcher
Parametric analysis
Wind tower
Passive cooling
Atmospheric boundary layer (ABL)

ABSTRACT

Windcatchers are used in building design as natural ventilation devices, providing fresh air supply and thermal comfort under suitable outdoor conditions. However, their performance is often constrained by environmental factors such as outdoor temperature, wind speed and direction. While passive or low-energy heating, cooling, and heat recovery devices have been integrated into conventional windcatcher designs, the impact of changing wind directions, which can render the windcatcher ineffective, is often not considered. Addressing this gap, this research builds upon a novel dual-channel windcatcher system. This system employs a rotary wind scoop to ensure a consistent fresh air supply and stale air exhaust, irrespective of wind direction and facilitates the integration of passive/low-energy technologies. Using a validated numerical computational fluid dynamics (CFD) model, the design of the proposed system was enhanced by incorporating technologies such as an anti-short-circuit device and wing walls, and modifications such as a larger wind scoop area and a redesigned wind cowl to increase the pressure differential between the inlet and outlet and reduce system friction. The modified windcatcher achieved a 28 % improvement in ventilation rate and outperformed a conventional four-sided windcatcher of the same size by up to 58 %. Furthermore, full-scale simulations of the building and windcatcher at varying heights were conducted under atmospheric boundary layer wind flow to provide a realistic assessment of the windcatcher's performance. This research contributes to the development of more efficient windcatcher systems for further passive technology integrations, enhancing their viability as sustainable ventilation solutions.

1. Introduction and literature review

With the development of the economy and living standards, the demand for improved indoor air quality in buildings has increased. Researchers are exploring new solutions to reduce energy consumption in the building sector due to rising energy prices and concerns about global warming [1]. The building sector directly and indirectly contributes to approximately 40 % of global carbon emissions, a percentage that is expected to rise to 50 % by 2050 [2,3]. Consequently, sustainable technologies aimed at curbing building energy consumption have been actively developed. These include the use of natural ventilation for passive cooling and the mitigation of indoor pollutants [4,5]. The importance of natural ventilation has been further emphasized following the COVID-19 pandemic, due to heightened concerns about airborne diseases and the need to remove viruses from indoor environments [6-8]. Additionally, as individuals spend increasingly longer hours working or residing within buildings, ensuring optimal indoor thermal comfort and maintaining high indoor air quality have become critical considerations. As buildings become more airtight, indoor pollutants cannot be removed through air leakage, and appropriate ventilation strategies are essential for modern buildings [9]. However, it is important to acknowledge that natural ventilation may not always provide satisfactory indoor thermal comfort under extreme external conditions characterized by excessive cold, heat, or humidity.

Consequently, conventional heating, ventilation, and air-conditioning (HVAC) systems are commonly used to maintain stable indoor thermal comfort. It is important to note that the energy consumption of HVAC systems can account for up to 50 % of a building's total energy use [10]. For example, in a city like Shanghai, the energy required for summer cooling can exceed 40 % of the total energy consumption [11]. Therefore, it is crucial to explore and develop energy-efficient cooling solutions, supporting the promotion of low-carbon development within the building industry [12].

Windcatchers are natural ventilation devices that not only improve energy efficiency but also enhance occupant well-being [13]. By installing windcatchers on rooftops, buildings can utilize prevailing winds to draw fresh air in and expel polluted air using wind pressure and thermal buoyancy [14,15]. While natural ventilation removes heat and in-

* Corresponding author.
E-mail addresses: jiaxiang.li@nottingham.ac.uk (J. Li), john.calautit1@nottingham.ac.uk (J. Calautit).

https://doi.org/10.1016/j.enbenv.2024.07.002
Received 12 May 2024; Received in revised form 2 July 2024; Accepted 3 July 2024
Available online xxx

Nomenclature

D	hydraulic diameter (m)
G_b	generation of turbulence kinetic energy due to buoyancy
G_k	generation of turbulence kinetic energy due to mean velocity gradients
p	pressure (Pa)
Re	Reynolds number
S_k	user defined source term for turbulence kinetic energy (m^2/s^2)
S_ε	user defined source term for energy dissipation rate (m^2/s^3)
t	time (s)
u	velocity (m/s)
Y_M	fluctuating dilatation in compressible turbulence to the overall dissipation rate
α_k	inverse effective Prandtl numbers for k
α_ε	inverse effective Prandtl numbers for ε
μ	dynamic molecular viscosity (Pa s)
ρ	density (kg/m^3)
τ_t	divergence of the turbulence stress

Abbreviations

ASCD	anti-short circuit device
CFD	computational fluid dynamics
HVAC	heating, ventilation and air-conditioning

door pollutants, thus ensuring favourable indoor thermal comfort and air quality, its effectiveness can be compromised under adverse outdoor conditions such as extreme temperatures and high humidity [16]. Specifically, high and low outdoor temperatures can lead to significant thermal discomfort [17]. Therefore, integrating passive or low-energy cooling and heating (for cold climates) technologies with the windcatcher system has become a significant area of research in natural ventilation [18,19]. Various passive technologies have been combined with windcatcher systems, including evaporative cooling in hot and dry climates [20-22], heat transfer devices for passive heat recovery [13,23], and earth-air heat exchangers to precool the supply air [24].

Wind direction significantly affects the functioning of these systems and can restrict ventilation [25-28] or thermal performance [29-32] if overlooked. Single-sided windcatchers perform well in regions with consistent wind direction but are less effective under variable wind conditions [14]. Additionally, the local wind environment in cities is often complex [33]. Evaluating the ventilation and thermal performance of such technology using fixed wind conditions, as done in wind tunnel experiments and CFD simulations, is inadequate for real-world applications where environmental conditions vary [34]. For instance, when integrating passive cooling and heating technologies into a multi-directional windcatcher [35,36], it's crucial to account for changes in the airflow direction within the air channels, as highlighted in the studies of [37-40].

1.1. The challenge and research gap

Fig. 1 illustrates a challenge identified in previous research regarding the impact of changing wind directions on a multi-directional windcatcher, which can capture wind flow regardless of the wind direction [31,41-44]. Positioning a cooling device in the channel facing the wind can enhance performance when the wind aligns with that side (Fig. 1 (a)). However, these cooling devices lose effectiveness if the wind shifts to the opposite direction or alters by 90° (Fig. 1 (b)). However, the effectiveness of the cooling device diminishes if the wind shifts to the opposite direction or changes by 90°. Installing cooling devices in both channels results in inefficiency, with one channel cooling the incoming air and the other unnecessarily cooling the extracted air (Fig. 1 (c)). This issue has often been overlooked in many studies using wind tunnel experiments and computational fluid dynamics (CFD) simulations, which typically assume constant and stable winds, unlike the variable conditions experienced [39,44-50].

Although numerous studies have explored the integration of passive cooling and heat recovery technologies in windcatchers [29,30,32,37,51], the majority have concentrated on the devices' ability to condition incoming air, with less attention to their performance under fluctuating wind conditions. However, the ability to operate reliably under various wind conditions is vital for the overall effectiveness of the building system [41,52]. For example, although evaporative cooling systems in windcatchers have shown promise, these systems have also been tested under static wind conditions, disregarding the impact of wind variability [21,53]. A few studies involving an evaporative cooling system in a single-sided windcatcher, complemented by a solar wall, revealed that variable wind directions could not only diminish ventilation efficiency but also lead to thermal discomfort from the reverse flow of solar-heated air [20,54].

Integrating passive heating, cooling technologies, or heat recovery devices can improve the thermal performance of windcatchers. Nevertheless, these enhancements are restricted by the limitations of either multi-directional or fixed windcatchers. Windcatchers with multiple openings are generally less affected by changes in wind direction and tend to maintain better overall ventilation efficiency compared to models with fewer openings, even though these may achieve higher peak ventilation rates under specific wind conditions [43]. Still, few research efforts have successfully achieved consistent ventilation and thermal performance in windcatchers that are independent of wind direction changes while incorporating passive or low-energy technologies. Some researchers have considered adding fans to ensure a continuous supply of fresh air at low wind speeds, but this approach compromises the windcatcher's zero-energy consumption and cost-effectiveness [55].

1.2. Research novelty, aim and objectives

To tackle the challenges associated with the variable performance of windcatchers under different wind directions and the constraints in integrating passive or low-energy technologies in traditional designs, we propose a novel dual-channel windcatcher. This design enables wind-driven natural ventilation that operates independently of wind direction, making it ideal for incorporating passive technologies [56]. As depicted in Fig. 2 and Video 1, the dual-channel windcatcher is designed to facilitate both the intake and expulsion of air within a space. It consists of two concentric ducts; the outer duct features a rotary wind scoop with a central aperture for the return duct. A vertical tail fin at the rear generates torque to rotate the wind scoop, ensuring it aligns with the prevailing wind. As a result, the outer duct consistently serves as the supply duct, utilizing the positive pressure created by the wind scoop, while the central chimney acts as the constant return duct, removing stale and warm air from the building. This configuration allows for efficient integration with passive or low-energy technologies, ensuring a continuous pathway for both supply and exhaust. In setups involving a cooling device, only the air in the supply channel is cooled. In contrast, in heat recovery systems, heat is continually transferred from the warm exhaust air to the fresh incoming air in the supply channel.

The present study aims to enhance the ventilation performance of the proposed system by implementing various strategies to augment the pressure differential between the inlet and outlet, thereby enabling the system to operate effectively even under low wind speed conditions. Achieving a higher ventilation rate is crucial, especially when integrating additional technologies that may introduce a pressure drop and reduce the airflow rate. The parametric analysis will focus on this objective without increasing the size of the windcatcher, while simultaneously enhancing ventilation efficiency and meeting the required ventilation demand within a smaller footprint. To accomplish this, the study will explore various design scenarios and operating conditions using a

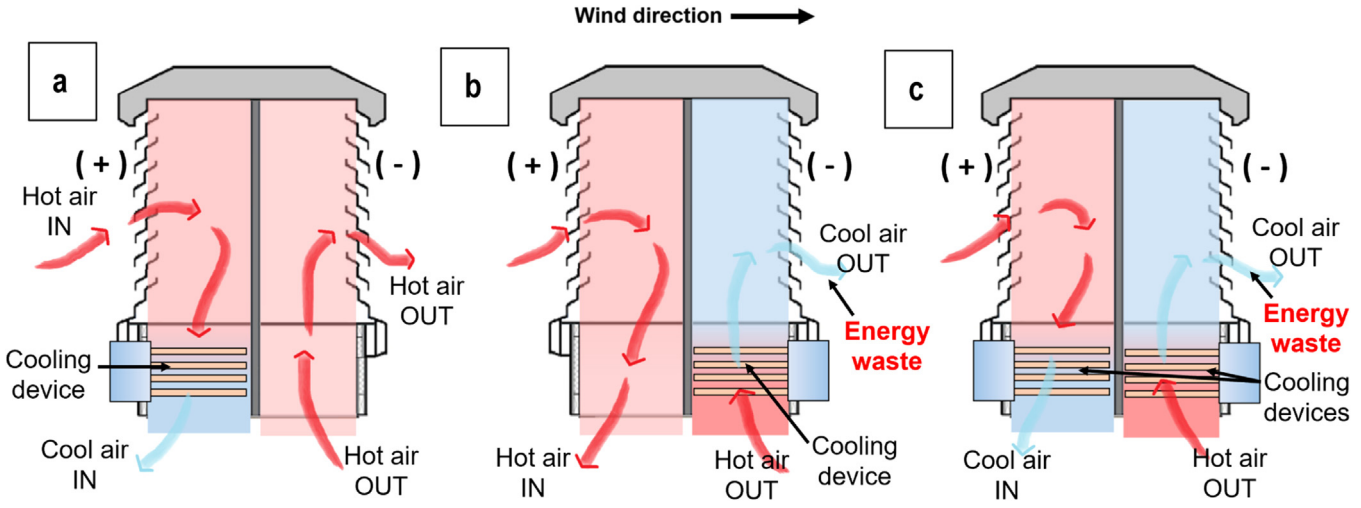

Fig. 1. Operation of a multi-directional windcatcher when the low-energy cooling device is in the (a) windward channel, (b) in the leeward channel, and (c) both channels.

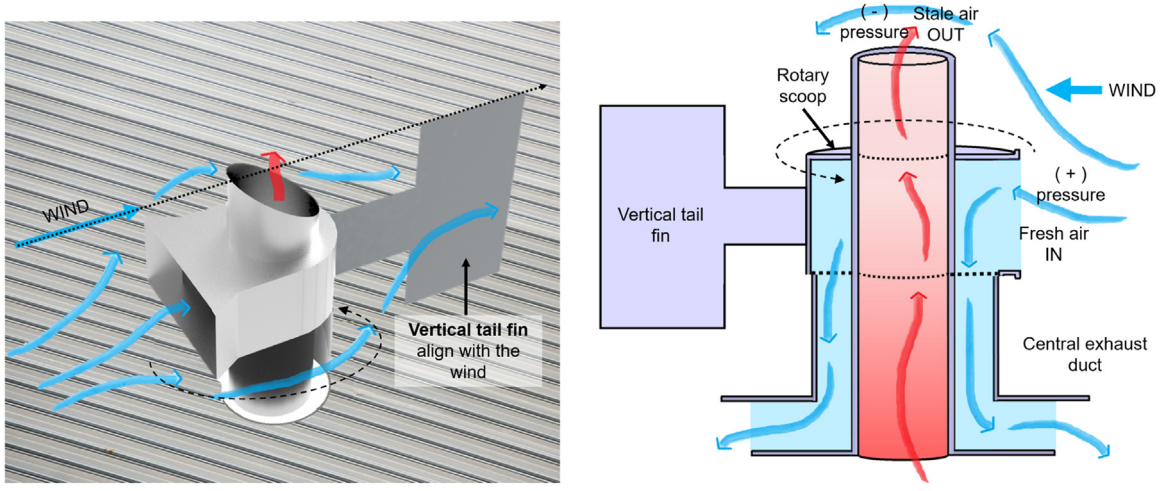

Fig. 2. Proposed rotary scoop windcatcher with dual channels for supply and exhaust streams.

numerical CFD approach, which will be validated experimentally. This combined methodology will accelerate the research process and help identify optimized solutions.

The parametric analysis of the proposed rotary dual-channel windcatcher will cover several key aspects: adjusting the diameter of the internal tube to achieve varying supply-to-return channel area ratios; implementing wing walls at the wind scoop inlet to generate higher positive pressure; modifying the height of the wind scoop inlet to optimize performance; chamfering the back of the chimney to create a wind cowl that facilitates increased air extraction; adjusting the height of the anti-short circuit device (ASCD) within the room to enhance airflow patterns; and modifying the height of the windcatcher tube while evaluating the influence of windcatcher height through comprehensive full-scale simulations. The refined parameters derived from this analysis will be applied to develop an optimized windcatcher model. This model's ventilation efficiency will then be benchmarked against that of a traditional four-sided windcatcher to evaluate its performance enhancements.

2. Method

The research flow diagram, depicted in Fig. 3, outlines the sequential progression of our study. By conducting this comprehensive evaluation, we aim to determine the improvements achieved through our optimization process and better understand the advantages of the proposed design over existing windcatcher configurations.

2.1. Dual-channel rotary windcatcher

The dual-channel rotary wind scoop windcatcher evaluated in this study is shown in Fig. 4. It included the following major components: a rotary component with a scoop inlet, a cowl outlet and a tailplane, the bearing and connection beam and the windcatcher foundation [44]. The present windcatcher device will incorporate a chamfered edge on the back side of the central chimney and wing walls at the entrance of the wind scoop to enhance the ventilation performance. The central chimney in the present design is also separated between the upper wind scoop and the lower section. This will combine the chimney outlet and wind scoop into a single component, replacing the initial prototype's ring-shaped bearing with a cost-effective bar-bearing design, reducing friction. As a result, the torque required to rotate the wind scoop and the size of the tailplane will be minimized. However, it should be noted that this aspect is not evaluated in numerical modelling.

Preventing down draught in a chimney is necessary for the ventilation system design to ensure the stale and warm air can be extracted from the chimney [47]. Fig. 2 and Video 1 illustrate the airflow directions within the windcatcher, where two concentric circular tubes create two distinct channels. With this dual-channel ductwork configuration

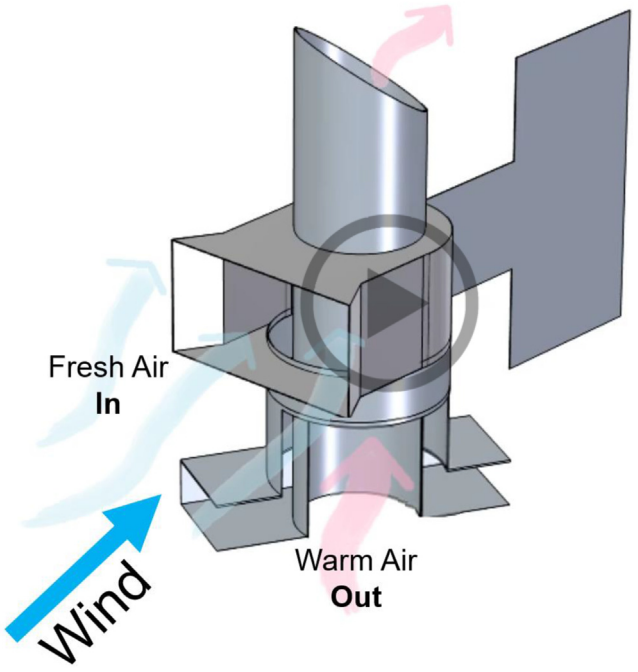

Video 1. Working mechanism of the proposed rotary scoop windcatcher with dual channels for supply and exhaust streams. *The video can be downloaded from the link in the Appendix section.*

and the presence of the rotary scoop, the external channel consistently functions as the supply channel, while the internal channel consistently serves as the return channel, irrespective of changes in wind direction. This setup facilitates a stable airflow, essential for seamless integration with passive technologies like passive heat recovery or cooling devices. The rotary component, beams and windcatcher foundation can be manufactured from stainless steel. This choice of materials ensures structural durability within the windcatcher system.

2.2. Experimental setup and testing

A cube-shaped test room with a length of 1.2 m was made from 50 mm thick insulation broad. Two L-shape anti-short circuit devices (ASCD) were added to avoid air short-circuiting and provide good air circulation inside the test room [57]. The windcatcher prototype is placed in the middle of the test room. A 4 m long blower-fan open wind tunnel with contraction, screen mesh and honeycomb flow conditioners [58] was made to provide a stable airflow for windcatcher ventilation rate testing. With the mesh screen and the flow conditioners, the turbulent flow from the industrial fans was stabilized to create uniform airflow which can be used for CFD model validation [44]. The wind speed profiles measured from the outlet of the wind tunnel were applied as the inlet of the CFD simulation and the wind speed profiles are presented in the Appendix (Table A1). The dimensions of the wind tunnel, test room, ASCD, and distance from the nozzle to the model are presented in Fig. 6 (c).

The dimension of the scaled experiment model is shown in Fig. 5. These dimensions were later modified to develop a full-scale model that would facilitate both ventilation performance evaluation and parametric analysis in the CFD simulations, as illustrated in Fig. 6. In this research, the size of the wind tunnel was constrained by the available space for the experiment, the necessity for uniform wind conditions, and the required wind speed, which in turn limited the size of the windcatcher. Our goal was to validate the numerical model with the experiment, ensuring that the same geometry was replicated in the numerical modelling work. The opening of the wind tunnel was positioned above the edge of the test room, setting the distance between the wind tunnel opening and the windcatcher inlet at 0.5 m.

Wind speeds were measured at 17 specific locations along the blower-fan open wind tunnel outlet. These measurements were employed in the validation CFD model as inlet wind speed. Due to the addition of screen mesh and flow conditioner, the maximum attainable wind speed was 3 m/s. After allowing the wind flow to stabilize and eliminate any instantaneous fluctuations, the average wind speed value for each measurement point was determined. To achieve a range of wind speed profiles under different average wind speeds, the fan was adjusted during testing. The wind speed profiles were measured for each test, ensuring an accurate representation of the actual wind speed profile across various average wind speeds. For wind speed measurements, the Testo 405i hot wire anemometer with an accuracy of $\pm$(0.1 m/s $\pm$5% of the readings) was employed and the experiments were tested under a room temperature of around 20°C. The same method was used to measure the airflow rate of the windcatcher, which will be compared with the CFD predictions. The results are presented in Section 3.1.

2.3. CFD modelling, grid verification and experimental validation

Computational Fluid Dynamics (CFD) is a cost-effective technique to perform numerical simulations and scrutinize an extensive volume of data pertinent to fluid dynamics. The CFD analysis has been deemed more beneficial compared to wind tunnel assessments for the exploration of specific attributes of windcatcher systems, including phenomena such as flow short-circuiting and recirculation, vortex regions, as well as supply and extract segments. Parametric analysis and model optimizations in CFD are preferable to wind tunnel experiments be-

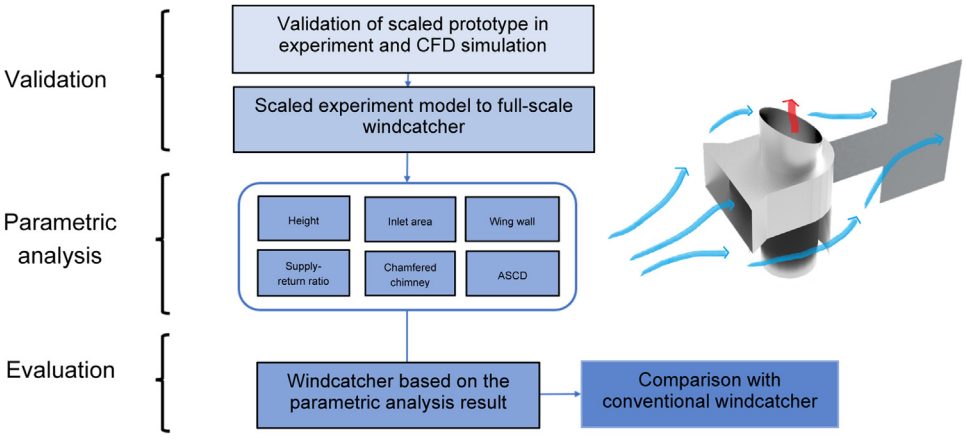

Fig. 3. Research process for the parametric analysis of the proposed rotary windcatcher.

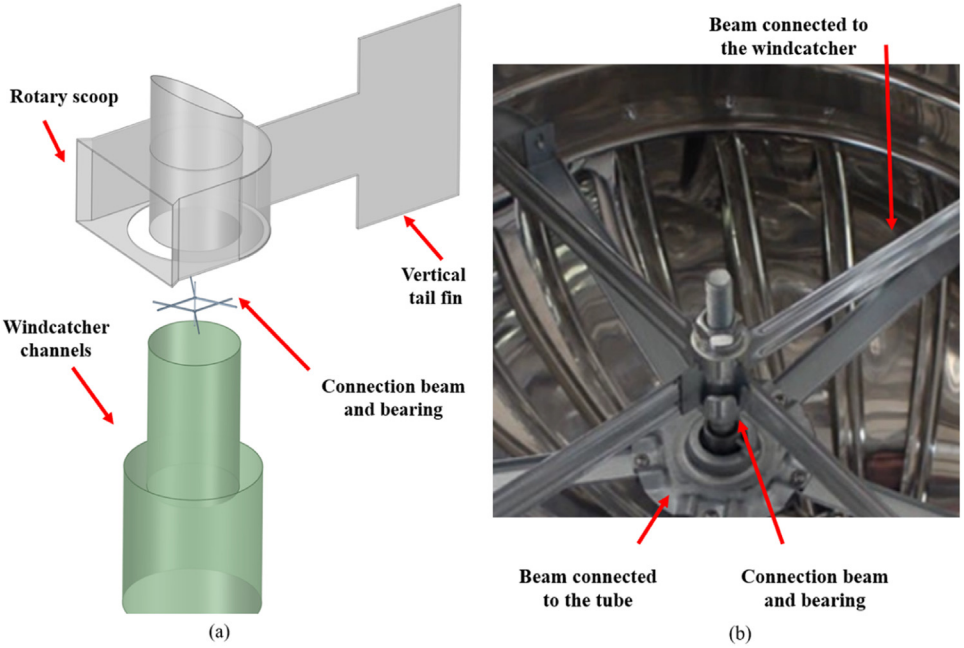

Fig. 4. (a) Components of the proposed dual-channel rotary scoop windcatcher, and (b) beams and bearing connecting the windcatcher and concentric ducts.

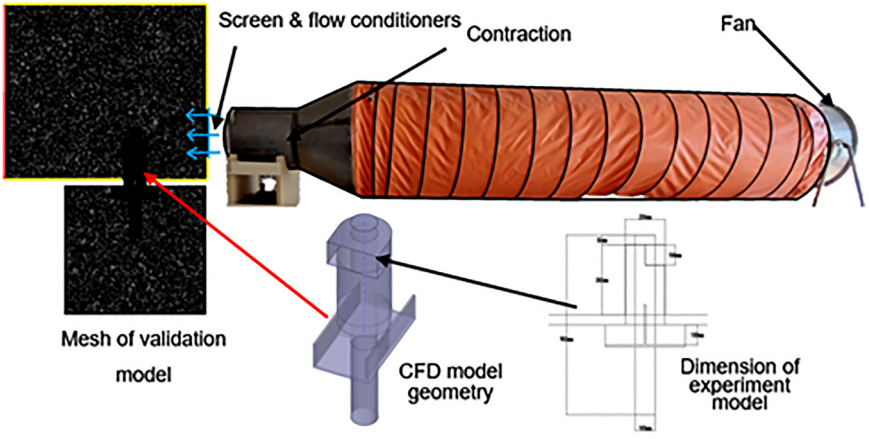

Fig. 5. CFD model (showing the meshed domain) which simulated the wind tunnel experiment setup.

cause controlling model geometry and environmental variables in CFD is more cost-effective and time-saving than manufacturing new experiment models. In this research, the commercial CFD software FLUENT was used to carry out the simulations of the windcatcher modifications for the parametric analysis [59]. The settings of CFD simulation are summarized in Table 1 [44]. The validation experiments were conducted under controlled conditions with a consistent environmental temperature and low wind speed. Therefore, assumptions were made that temperature variations would not occur within the CFD simulations. Our research primarily focused on airflow and ventilation performance within the windcatcher, consequently, we solely solved the mass and momentum equations to examine these aspects. The governing energy equation was excluded to simplify the process, as it was not applicable to heat transfer or internal heat sources within the building.

The Reynolds-averaged Navier-Stokes, k-epsilon RNG equations and semi-implicit method for pressure-linked equations segregated pressure-based algorithm were utilized [60], and the second-order upwind scheme was employed to discretize all the transport equations. The governing equations for the mass (Eq. (1)), momentum (Eq. (2)), and k and epsilon (Eq. (3) and Eq. (4)) [61] are detailed below:

$$\frac{\partial \rho}{\partial t} + \nabla \times (\rho u) = 0 \tag{1}$$

Table 1
CFD settings and boundary conditions.

Term	Value and settings
Inlet	
Velocity (m/s)	0–3 (wind speed profile based on wind tunnel), 1–7 (wind speed for parametric analysis)
Initial Gauge pressure (Pa)	0
Specification method	k-epsilon RNG
Outlet	
Gauge pressure (Pa)	0 (atmospheric)
Wall	
Shear condition	No slip
Roughness height	0
Roughness constant	0.5
Converged residuals	
Continuity / k / Epsilon	0.001
X/Y/Z velocity	0.0001

where u refers to the fluid velocity vector, t is time, and ρ is density.

$$\frac{\partial \rho}{\partial t} + \nabla \times (\rho u \nabla u) = -\nabla p + \rho g + \nabla \times (u \nabla u) - \nabla \times \tau_t \tag{2}$$

where g is a vector of gravitational acceleration, p is the pressure, τ_t is the divergence of the turbulence stresses, and μ is dynamic molecular

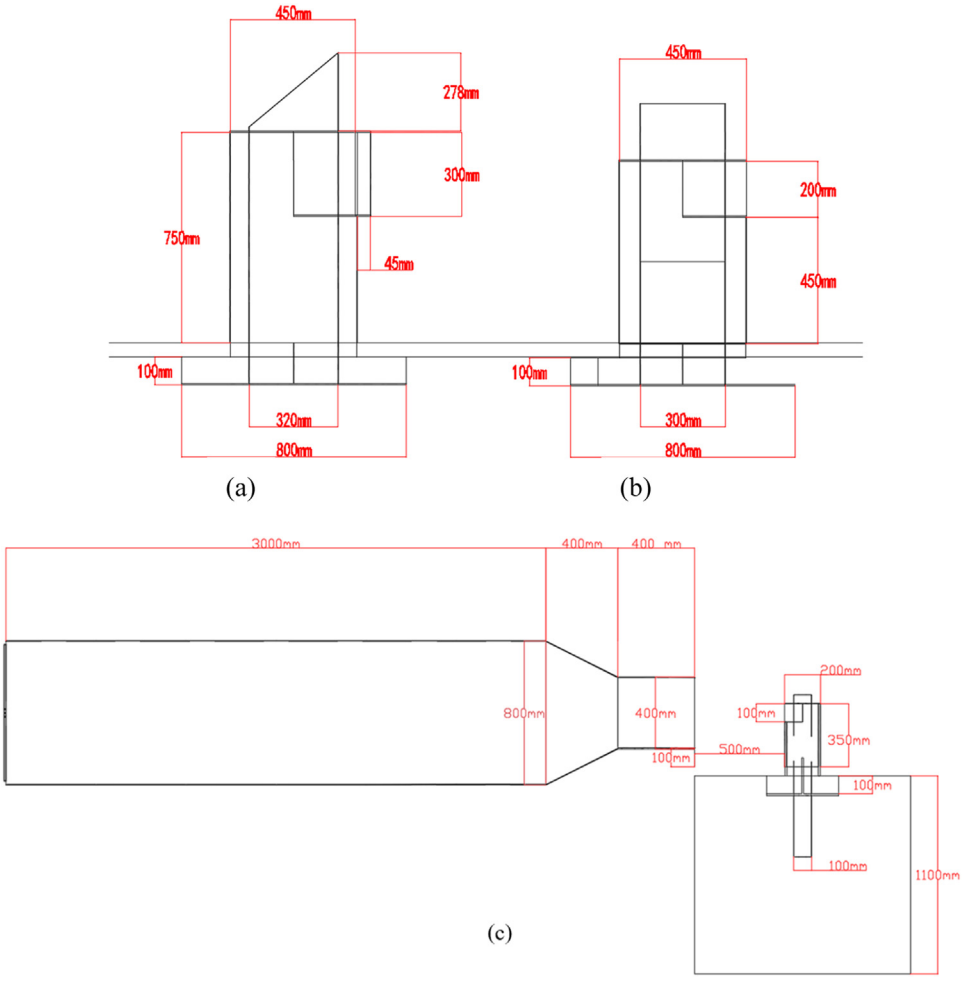

Fig. 6. Dimension of the full-scale model of the (a) initial and (b) final rotary scoop windcatcher, and (c) dimension of the wind tunnel and experimental model.

viscosity.

$$\frac{\Delta}{\delta t}(\rho k) + \frac{\delta}{\delta x_i}(\rho k u_i) = \frac{\delta}{\delta x_i}\left(a_k \mu_{eff} \frac{\delta k}{\delta x_j}\right) + G_k + G_b - \rho\varepsilon - Y_M + S_k \quad (3)$$

$$\frac{\Delta}{\delta t}(\rho\varepsilon) + \frac{\delta}{\delta x_i}(\rho\varepsilon u_i) = \frac{\delta}{\delta x_j}\left(a_k \mu_{eff} \frac{\delta\varepsilon}{\delta x_j}\right) + C_{1\varepsilon}\frac{\varepsilon}{k}(G_k + C_{3\varepsilon}G_b) - C_{2\varepsilon}\rho\frac{\varepsilon^2}{k} - R_\varepsilon + S_\varepsilon \quad (4)$$

where *Gb* and *Gk* represent the generation of turbulence kinetic energy due to buoyancy and mean velocity gradients. Y_M defines the overall dissipation rate. α_k and α_ε are the inverse effective Prandtl numbers for k and ε. S_k and S_ε are user-defined source terms.

The mesh independence analysis of the optimized model is shown in Fig. 7, utilizing different mesh sizes including coarse (2.6 million element number), medium (6 million element number) and fine (11 million element number). As the research focuses on the ventilation performance of the windcatcher, the ventilation rate of the model with different mesh sizes was simulated and compared. As observed, all the models achieved identical simulation results. The ventilation rates across models with varying mesh qualities were consistent. However, a medium-mesh quality was chosen to provide a balance between computational efficiency and precision. For instance, the vector plot distribution in the accompanying figure exhibits greater uniformity with the medium mesh compared to its coarser counterpart.

2.4. Proposed windcatcher parametric analysis

To enhance the ventilation rate, this research focused on parametric analysis by adjusting various factors. However, the evaluation did not involve assessing the ventilation performances of windcatchers with different cross-section areas [62]. Instead, the modifications were tested using models with identical cross-section areas. The adjustments included modifying the supply-to-return channel area ratio, incorporating wing walls with varying angles and lengths at the wind scoop inlet, adjusting the height of the wind scoop inlet, chamfering the back of the chimney at different angles, modifying the height of the ASCD within the room, and evaluating the impact of windcatcher height through ABL wind simulations. These modifications aimed to identify the most effective design parameters for enhancing the ventilation rate and improving the overall performance of the windcatcher system.

2.4.1. Supply-to-return channel area ratio

The turbulent airflow in the ventilation duct was affected by the Reynolds number in the duct and the roughness of the surface [63]. The area and shape of the channels would affect the hydraulic diameter of the system which would affect the turbulence and the Reynolds number in the duct. The Fanning friction factor f can be used for the turbulent flow calculation [64,65] which was increased by the increase of Reynolds number. Thus, adjusting the shape and area of the supply and return channels to achieve a lower hydraulic diameter was necessary to decrease the Reynolds number and the system friction. In this research, lower system friction was achieved by adjusting the diameter ratio of supply and return channels to minimize overall system friction

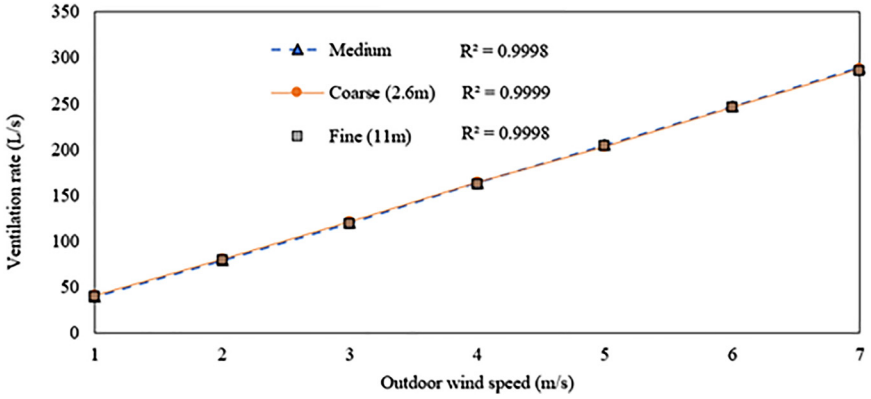

Fig. 7. Mesh independence analysis.

rather than decrease the friction in a single channel. The diameter of the internal tube was adjusted up to 450 mm to evaluate the ventilation performance with a different supply-to-return ratio.

$$Re = \frac{\rho u D}{\mu} \tag{5}$$

where *Re* is the Reynolds number of the system; u is the velocity of airflow in the system in m/s; D is the hydraulic diameter in m; ρ is the density of the liquid in kg/m^3; μ is the viscosity of the liquid in Pa*s.

2.4.2. Wing walls at the inlet

The implementation of wing walls has been recognized as an effective natural ventilation device for enhancing the performance of single-side ventilation [66]. Adding a wing wall could provide a sharp edge at the inlet, which increases pressure, thereby improving ventilation performance [67,68]. By adding the wing walls to the rotary wind scoop components, the inlet area can also be increased to capture more airflow and further improve ventilation performance. Thus, wing walls with different angles, from 0° to 90°, and lengths, from 50 mm to 200 mm, at the wind scoop inlet were investigated, as shown in Fig. 9 (a).

2.4.3. Wind scoop inlet height

Increasing the area of the windcatcher opening is a highly effective approach for enhancing airflow within a windcatcher. However, it is important to note that the benefits of increasing the opening area become limited once it reaches an excessively high level. In light of this, the present study explored an alternative avenue for improving the ventilation rate by adjusting the height of the wind scoop inlet. This investigation sought to determine whether increasing the height of the wind scoop proved to be a cost-effective method for enhancing the ventilation rate. The range of wind scoop heights examined spanned from 0 mm to 500 mm, as depicted in Fig. 9 (b). By analyzing the impact of varying wind scoop heights, this research aimed to identify an optimal height that would yield the desired improvements in ventilation rate while considering practicality and cost-effectiveness.

2.4.4. Chamfering the back of the chimney

Chimneys play a crucial role in extracting polluted air from buildings, and their performance remains unaffected by the wind direction, making them suitable components for multi-directional windcatcher designs. However, the performance of a chimney in a fixed design does not fully leverage the advantages of a rotary scoop windcatcher, where the chimney component is installed within a rotating device capable of always facing the wind. As a result, the ventilation rate achievable in the current design is not maximized. To address this limitation, a new approach involving the chamfering of the chimney was explored, as illustrated in Fig. 9 (c). By incorporating a chamfered angle, a pressure cowl was created, allowing the wind to be redirected with the assistance of the tail fin. This design modification generated a larger negative pressure at the outlet, enabling the extraction of a greater volume of air. Consequently, this research focused on investigating and comparing the ventilation performance of chamfered chimneys with varying angles, ranging from 0° to 60°. Through this analysis, we aimed to identify the most effective angle for maximizing the ventilation performance of the windcatcher system.

2.4.5. Impact of atmospheric boundary layer (ABL) upstream wind

The evaluation of the windcatcher's ventilation performance in existing studies has mostly been conducted in wind tunnel-based domains and under uniform wind conditions, rather than with a full-scale building and under atmospheric boundary layer (ABL). It is important to note that the presence of a building's edges can significantly influence the wind speed profile above the structure, and the wind speed near the roof may be substantially lower than the undisturbed outdoor wind at the same height. Consequently, it becomes necessary to increase the height of the windcatcher adequately, considering the geometry of the building, to effectively capture the wind for a fresh air supply.

However, it is crucial to recognize that the total pressure loss within the windcatcher system is influenced by factors such as friction and total length. Therefore, as this research primarily focuses on the parametric analysis of windcatcher geometry, it is imperative to investigate the impact of tube length as well. This analysis aims to ensure that the windcatcher system meets the requirements of real-world applications and effectively caters to the ventilation needs of buildings. By considering both the height and tube length, we can optimize the windcatcher design to achieve optimal performance in practical scenarios.

2.4.6. Height of the ASCD

In order to address potential issues related to the short-circuiting of supply air, an anti-short circuit device (ASCD) was integrated directly beneath the windcatcher. This configuration aims to forestall any possible rerouting of the ventilation airflow directly from the supply to the exhaust, bypassing the intended air distribution in the room, a phenomenon known as "short-circuiting". In addition to the installation of the ASCD, a thorough examination was conducted to discern the effect of the device's height within the room on the rate of ventilation. The objective of this assessment was to find an optimal balance between the ASCD's dimensions and the ventilation rate, a crucial step towards maximizing material efficiency. This ensures a sustained high-performance level of the ventilation system without unnecessary expenditure on oversized ASCDs.

The efficacy of the windcatcher was scrutinized under a variety of conditions. Initially, its performance was evaluated at both its original and modified heights, under a constant wind speed setting. This evaluation allowed for an understanding of the windcatcher's performance, independent of wind speed fluctuations. Further evaluation was conducted under more realistic, full-scale conditions that encompassed an atmospheric boundary layer wind speed profile.

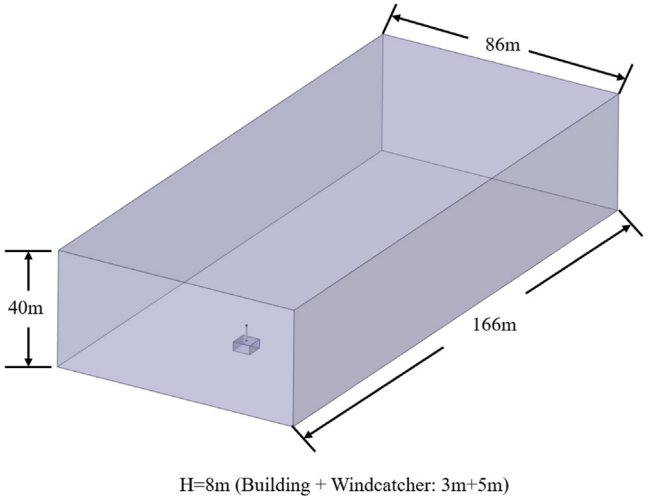

Fig. 8. Dimension of computational domain utilized for the full-scale simulation.

The full-scale CFD simulation domain size (Fig. 8) and the atmospheric boundary layer were determined based on guidelines from [52], encompassing dimensions of 5 times the height (5*H*) in front, 5*H* on the sides, 5*H* above and 15*H* behind the building. In this research, *H* is 8 metres, corresponding to the height of the tallest model. With a mesh size of 0.5 m in the domain and 0.008 m around the windcatcher and building surface, the maximum mesh element number of the full-scale simulation was about 28 million.

In the full-scale simulation with the atmospheric boundary layer, the wind speed at the windcatcher's height level was 5 m/s and the wind speed profile was 6 x $(H/15\ \text{m})^{0.143}$. A pitched, curved, and domed roof building can be a solution to avoid the impact of the building edge [69,70]. Thus, a full-scale simulation of the windcatcher with a pitched roof was also applied to investigate the impact on the ventilation rate.

All the parametric analyses (Fig. 9) were conducted based on the initial windcatcher model with a 450 mm external diameter with an identical outdoor wind speed of 5 m/s, and the refined parameters were combined for the final optimized windcatcher.

2.5. Comparison with the conventional 2-sided & 4-sided windcatcher

The primary objective of this parametric analysis is to enhance the ventilation performance of the rotary wind scoop windcatcher, with a specific focus on achieving a higher ventilation rate compared to existing models. This analysis is key to advancing our understanding of how variations in design parameters can affect the windcatcher's overall performance, particularly in terms of its ability to facilitate air circulation within the enclosed space it services. Once the parametric analysis of the initial rotary wind scoop windcatcher was completed, it was crucial to gauge the effectiveness of these adjustments. This was accomplished by comparing the ventilation rate of the initial and modified versions of the rotary scoop windcatcher. To ensure a fair and balanced evaluation, the comparison was made against the conventional two and four-sided windcatcher that maintained an identical area and opening height.

3. Results and discussion

3.1. Model validation

The CFD simulation model was validated against the wind tunnel data for the total ventilation rate, as illustrated in Fig. 10. Through these multi-faceted evaluations, a linear correlation was established between the average environmental wind speed, as recorded in the wind tunnel, and the total ventilation rate facilitated by the windcatcher. In the

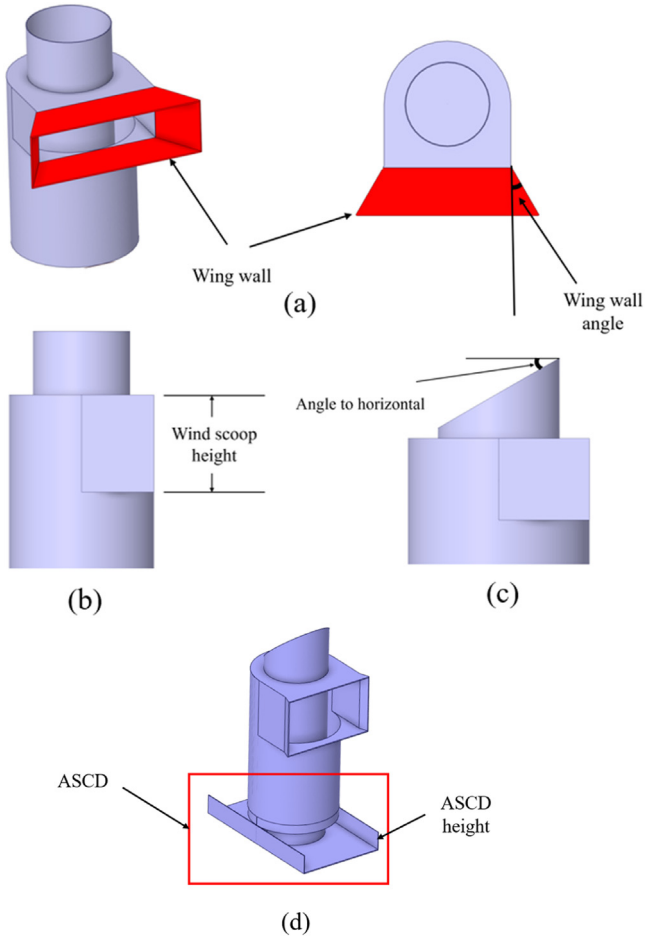

Fig. 9. Parametric analysis of (a) wing wall at the wind scoop inlet, (b) wind scoop height, (c) chamfered chimney, and (d) ASCD and height.

scaled-down prototype, the fresh air supply ranged between 1.7 L/s/m^2 and 9.18 L/s/m^2. This performance metric correlated with outdoor wind speeds varying between 0.5 m/s and 2.5 m/s, thus demonstrating the prototype's sensitivity and responsiveness to the ambient wind conditions. During these investigations, a certain disparity was noted between the average ventilation rates derived from the CFD simulation and the experimental results. The difference was quantified to be approximately 0.156 L/s/m^2, which translated into an average percentage deviation of 4.5 %. This discrepancy, while minor, underscored the inherent challenges in perfectly simulating the complex physics of fluid dynamics and the effect of real-world variables.

In response to these findings, modifications were implemented within the scaled experimental model to facilitate the creation of a full-scale version. The results of the simulation models were compared, and while small variations were observed between the different simulation methods, a similar trend was observed. The wind speed validation points and validation results are shown in Fig. 11, in the vertical plane in the middle of the model. Validation point 1 was 1 cm above the bottom of the ASCD and 20 cm to the centre of the tubes. Validation point 2 was 5 cm away from the wall and 55 cm above the room's floor. The centre wind speed point was in the middle of the return duct, with a height of 5 cm above the top surface of the test room.

3.2. Supply-to-return channel area ratio

The impact of the supply-to-return channel area ratio on the ventilation rate was assessed and shown in Fig. 12. The percentage ratio was calculated by the new ventilation rate divided by the initial venti-

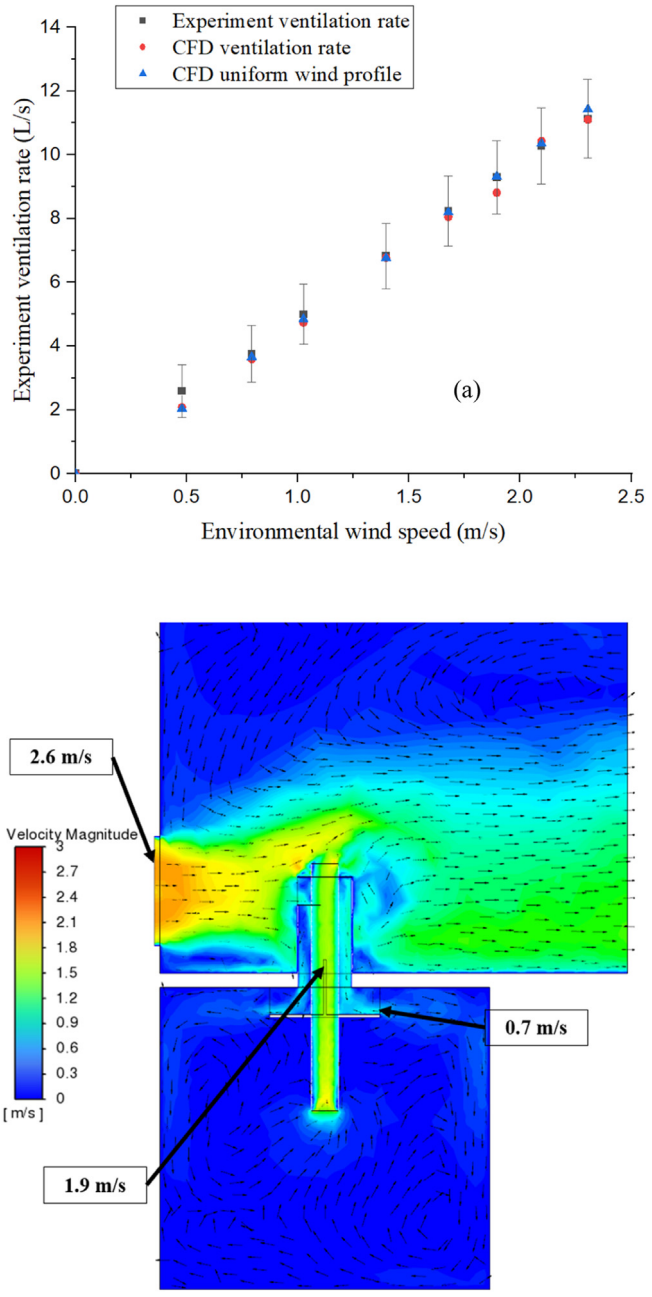

Fig. 10. (a) Comparison between experiment and CFD results, and (b) cross-sectional contour showing the airflow velocity distribution around the validation model.

lation rate. It was observed that achieving an optimal ventilation rate required equivalent areas for both the supply and return channels. Deviations from this balanced ratio resulted in significant alterations in the wind speed within the channels, subsequently leading to varying levels of pressure loss. For instance, when the supply channel area was considerably smaller than that of the return channel, a substantial increase in wind speed was observed within the supply channel. This, in turn, escalated the pressure loss within the system. Similar consequences were noted when the area of the return channel was reduced.

By ensuring that the areas of the supply and return channels were identical, a balanced ventilation configuration was achieved. In such cases, the wind speeds designed for both channels were equal, thus minimizing pressure loss within the system while maintaining a constant ventilation rate. Consequently, it became evident that an unbalanced supply-to-return channel ratio could significantly impact the overall ventilation rate within the room.

Furthermore, the diameter of the ducts played a crucial role in determining the ventilation rate. The final optimized model demonstrated that a balanced duct diameter of 320 mm yielded the highest ventilation rate when considering a constant diameter. However, it is important to consider the manufacturing costs associated with producing a windcatcher with a specific diameter. Opting for a ready-made product available in the market, such as 300 mm or 400 mm, may prove to be a more cost-effective solution, despite potential slight deviations from the ideal diameter.

To minimize any discrepancies in the area difference between the supply and return channels, it is recommended to maintain a ratio of approximately 0.707 between the internal and external diameters. This approach helps to achieve a more balanced airflow distribution and enhances the overall efficiency of the windcatcher system.

3.3. Wing wall angle and length

The impact of both the angle and length of the wing wall on the ventilation rate has been meticulously examined and is graphically depicted in Fig. 13. It was observed that all the windcatchers equipped with wing walls outperformed the original model in terms of ventilation performance.

In scenarios where the angle of the wing wall was less than 50°, it was found that shorter wing walls led to an enhanced ventilation rate. This can be attributed to the fact that introducing a lengthy wing wall under low-angle conditions essentially extended the supply channel's length without increasing the wind scoop's area. This caused an upsurge in pressure loss without a corresponding increase in air capture, an unfavourable outcome for ventilation efficiency.

Low-angle wing walls at the wind scoop inlet could generate an extended sharp edge outside the windcatcher foundation, thus amplifying the ventilation rate at the front. However, a longer wing wall did not contribute to a more significant increase in the ventilation rate when compared to a shorter one. As a result, models fitted with shorter wing

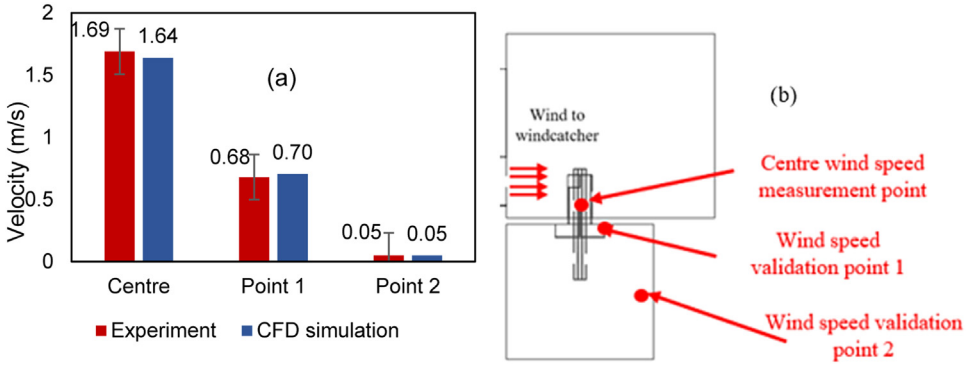

Fig. 11. (a) Result of three wind speed validation points, and (b) location of three wind speed validation points.

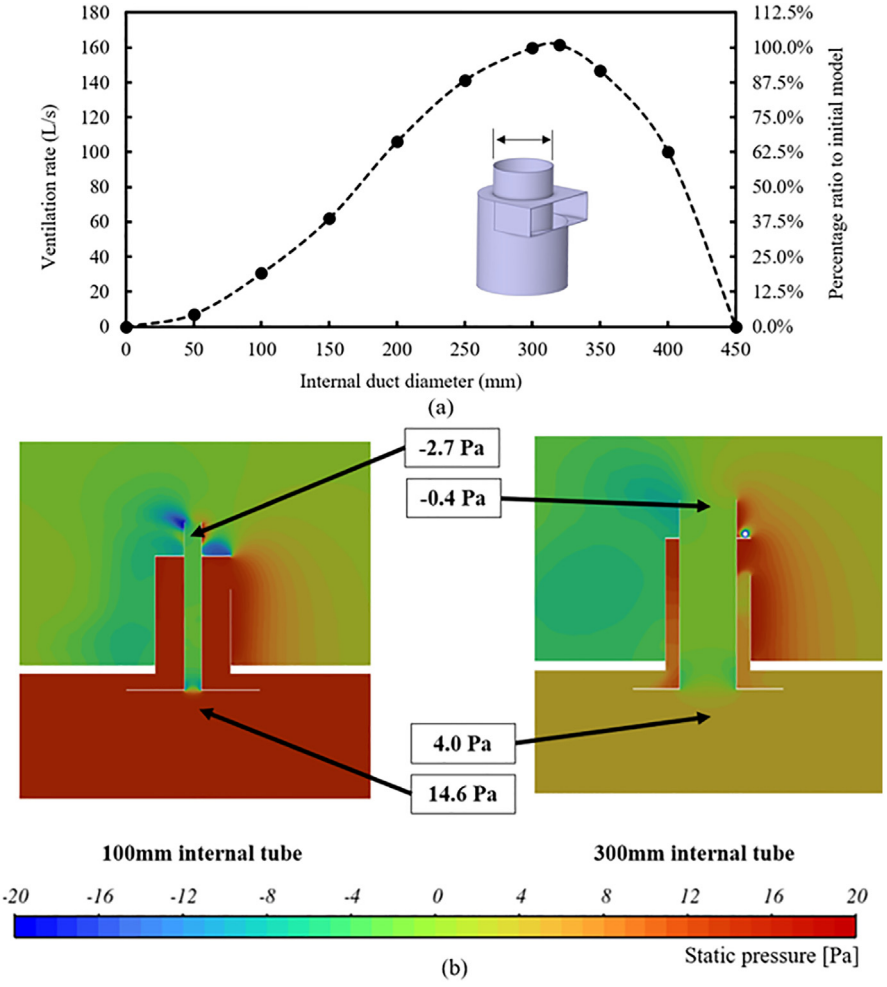

Fig. 12. (a) Impact of the internal duct diameter on the ventilation rate at 5 m/s outdoor wind speed, and (b) cross-sectional pressure contour comparing two designs.

walls achieved a higher ventilation rate relative to those with longer wing walls.

In contrast, for larger angles exceeding 50°, increasing the length of the wing wall essentially expanded the inlet area. Consequently, windcatchers with longer wing walls demonstrated superior ventilation performance in comparison to their counterparts with shorter wing walls.

However, it is essential to consider the practical implications of extending the wing wall, as it inherently increases the size of the wind scoop. A wind scoop that is substantially larger than the windcatcher channel may not present a cost-efficient solution compared to simply opting for a larger-diameter windcatcher. As such, while a 200 mm wing wall with an 80-degree angle could potentially reach the maximum ventilation rate, a more pragmatic and efficient design, considering material usage and spatial constraints, was found to be a 50 mm wing wall with a 20-degree angle. This design managed to strike a balance between achieving an optimal ventilation rate and maintaining cost and space efficiency.

3.4. Height of wind scoop and anti-short circuit device (ASCD)

The area of wind capture in a windcatcher constitutes a crucial determinant of its ventilation efficiency. The effect of modifying the height of the wind scoop on the ventilation rate was examined, with the results shown in Fig. 14. An increase in the ventilation rate was noted when the height was increased to 200 mm. This boost is largely attributable to the considerable system friction and a diminished frontal area for wind capture associated with a small inlet opening. Nonetheless, once the area of the wind scoop was expanded to approximately twice that of the supply channel area, the subsequent improvement in the ventilation rate was negligible. This observation indicates that despite further enlargements of the wind scoop area beyond 300 mm, the pressure differential created by the wind was inadequate to provide additional airflow through the system. When analyzing improvements in the ventilation rate, a height increment from 200 mm to 300 mm led to an estimated increase of approximately 12 %. Conversely, doubling the height of the wind scoop from 200 mm to 400 mm only resulted in a relatively modest 15 % increase under identical environmental wind conditions. Hence, a height increase of the wind scoop to 300 mm was determined to be the ideal strategy for ventilation enhancement. This adjustment not only ensured a high ventilation rate but also promoted more efficient material usage, which is crucial in striking a balance between enhancing performance and reducing material/resource consumption.

As shown in Fig. 14 (a), the results indicated that after reaching a height of 100 mm, the ventilation rate demonstrated a near-constant trend. This plateau effect in the ventilation rate beyond the 100 mm mark underscores the importance of this particular ASCD height in the ventilation performance of the model. The velocity contour and vector of windcatcher with different ASCD heights are presented in Fig. 14 (b). The model with a 100 mm ASCD height had a better distribution of the airflow on both sides compared with the model with 200 mm ASCD height. Based on these findings, the initial ASCD height of 100 mm was retained for further investigation. This was rooted in the understanding that any increase in height beyond this threshold would not significantly enhance the ventilation rate. Thus, maintaining the ASCD at this height aligns with the principle of optimization – achieving the highest possible ventilation performance while minimizing unnecessary

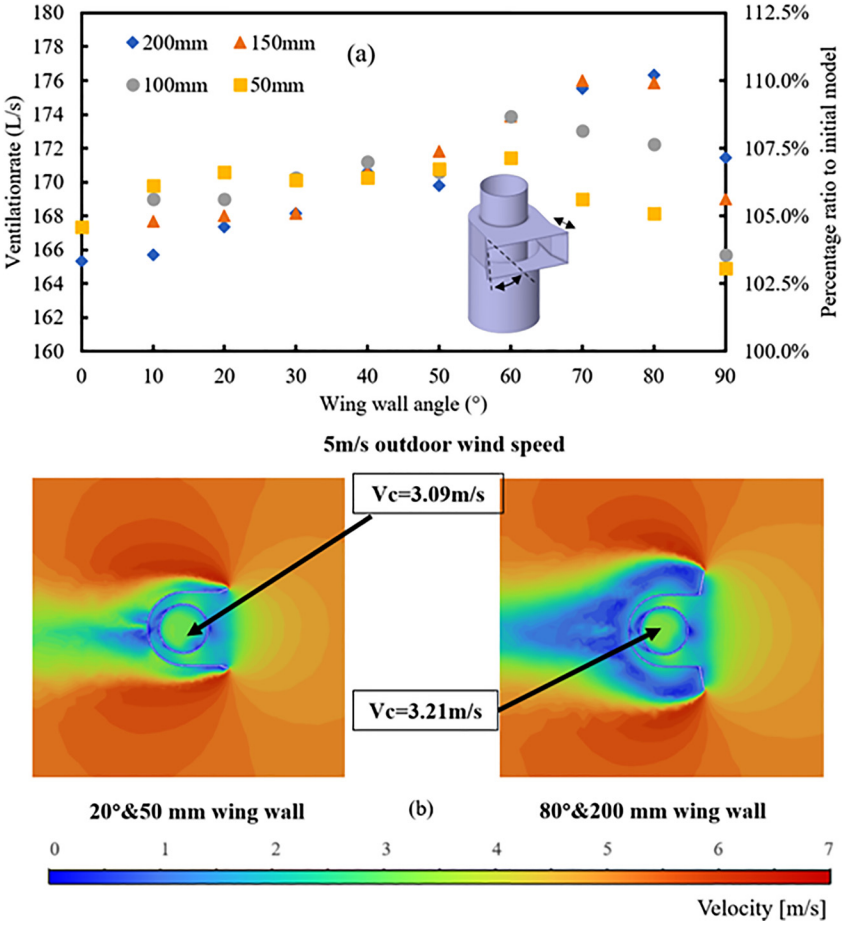

Fig. 13. (a) Impact of the wing wall angle on the ventilation rate at 5 m/s outdoor wind speed, and (b) horizontal cross-sectional velocity contour comparisons.

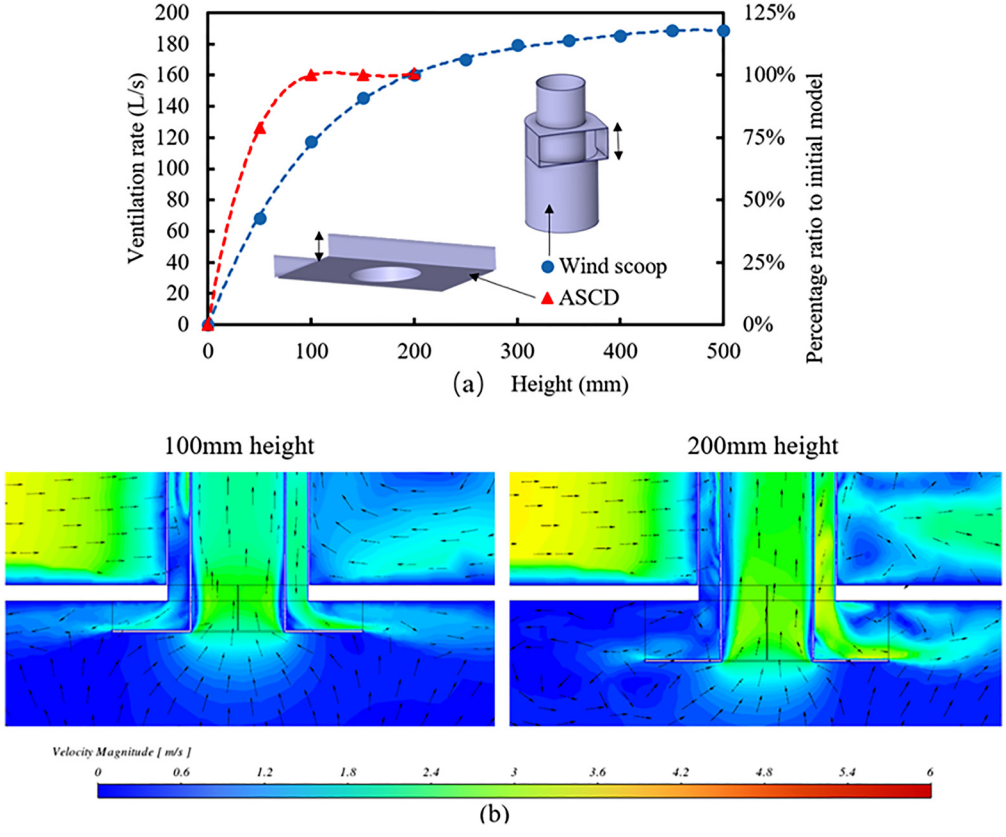

Fig. 14. (a) Impact of wind scoop height on the ventilation rate at 5 m/s outdoor wind speed, and (b) cross-sectional velocity contours and vectors comparing wind-catchers with different ASCD heights.

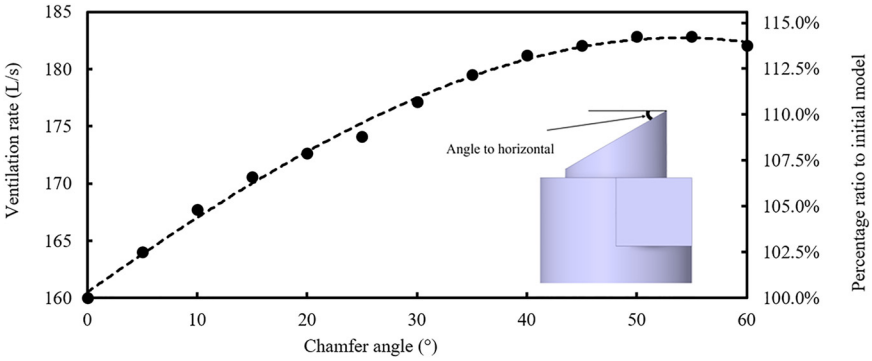

Fig. 15. Impact of the chamfered chimney angle on the ventilation rate at 5 m/s outdoor wind speed.

material consumption and spatial requirements. This investigation into the influence of ASCD height exemplifies the holistic approach taken in this study, where every variable, no matter how ostensibly minor, is examined for its potential impact on the overall performance of the windcatcher system. The ventilation performance of the windcatcher with and without ASCD was also evaluated by CFD simulation. After applying the ASCD, the air escaping the building without circulating inside the room was significantly reduced. The airflow distribution in the building was more uniform after applying the ASCD, and the supply and exhaust streamline were separated into different directions.

3.5. Chamfered chimney angle

Incorporating a chamfered chimney outlet can facilitate an increase in the outlet area at the region of negative pressure, whilst concurrently generating a larger zone of negative pressure behind the outlet to promote increased extraction of air from the room. Within a model featuring a rotary wind scoop, the outlet chimney could be affixed to the wind scoop, enabling simultaneous rotation. This ensures that the wind scoop constantly faces the wind, and the chamfered chimney maintains its optimal orientation without the need for electrical power.

As presented in Fig. 15, the introduction of a chamfered chimney enhanced the ventilation performance of the initial windcatcher, with the ventilation rate continuing to rise in line with the angle of the chamfer. However, the ventilation rate tended to stabilize once the chamfered angle reached approximately 45°, peaking around a 50° chamfered angle, which resulted in a ventilation rate improvement of about 14 %. The requirement for a high chimney becomes significant for a large chamfer angle exceeding 45°, leading to a considerable rise in material needs, yet the ventilation rate ceases to increase with further chamfered angle increments past 45°. Consequently, a chimney cut angle of 40° was selected for the final model.

3.6. Windcatcher height and full-scale simulations

The unique sharp edge of a flat roof building, when oriented perpendicularly to the wind direction, creates turbulent airflow above the roof surface. This turbulence, in turn, causes the wind speed profile near the building's edge in actual operational conditions to deviate substantially from those observed under controlled experimental settings, which will be accelerated and separated by the building edge [71,72]. Consequently, even though the wind speed at the height of the windcatcher in the atmospheric boundary layer is equal to the uniform wind speed in the numerical simulation and experiment, the ventilation performance of the windcatcher in a real building might be totally different to the prediction achieved by the wind tunnel experiment or the uniform wind speed simulation. To better understand these performance variations, comparisons were drawn between full-scale simulations and those under a uniform environmental wind speed.

As depicted in Fig. 16, the windcatcher of initial height was strategically situated at the centre of the roof, in close proximity to the roof's surface. In the full-scale simulation, the wind speed in the immediate vicinity of the windcatcher was nearly reduced to zero, leading to a near-zero ventilation rate. However, the ventilation rate in the full-scale simulation showed a significant increase when the height of the windcatcher was increased from 0.5 m to 1 m and thereafter, it maintained a state of equilibrium.

In contrast, under unvarying wind speed conditions in the absence of a building, the performance of the windcatcher was unaffected by the turbulence at the building edge. As a result, it demonstrated a gradual decline in response to increases in windcatcher height, mainly due to the escalating system friction. Nevertheless, the sharp edge of the building amplified the wind speed above the initial windcatcher, thereby enabling a taller windcatcher to harness the wind with a significantly greater velocity. Therefore, despite a reduction in ventilation rate due to the expanded tube length in a taller windcatcher system, the overall ventilation rate of this system still exceeded that of the initial model under constant environmental wind speed conditions.

Moreover, extending the tube length by 3 m resulted in a 10 % decrease in the total ventilation rate. The increase in tube length can expand the area available for sunlight capture, potentially proving beneficial for solar chimneys or other passive technologies such as heat recovery. This finding suggests a multi-faceted approach to building design that considers the interplay between wind and solar energy, offering insights for the enhancement of both ventilation and energy efficiency.

In the full-scale simulation, the windcatcher of initial height, when incorporated into a pitched-roof building, exhibited ventilation rates that were essentially on par with those observed under a constant environmental wind speed profile. This can be primarily attributed to the fact that the horizontal wind speed profile in the immediate vicinity of the windcatcher remained remarkably stable, largely impervious to the influence exerted by the building's roof geometry. This unimpeded wind profile allows for more consistent wind-driven ventilation, closely mimicking conditions of a constant environmental wind speed.

In the context of the windcatcher geometry, the design process did not specifically optimize for tube length. Instead, it was recognized that the tube length would play a critical role in the windcatcher's performance, impacting factors such as wind capture, pressure differentials, and system friction. However, considering the intricate balance between these variables and the potential material and cost implications of an elongated tube, a decision was made to retain the initial tube length for the final geometry optimization phase. Maintaining the initial tube length allowed for a focus on optimizing other elements of the windcatcher's design in the current stage of research. Meanwhile, the implications of varying tube lengths, such as changes in system friction and wind capture, can be considered in future investigations. This approach affords a more nuanced and measured design process that can better adapt to diverse architectural contexts and environmental conditions.

3.7. Combined modifications evaluation

The parametric analysis provides insights into which components of the windcatcher system have the most significant impact on ventilation rates, as shown in Table 2. Among the parameters tested, the chamfered

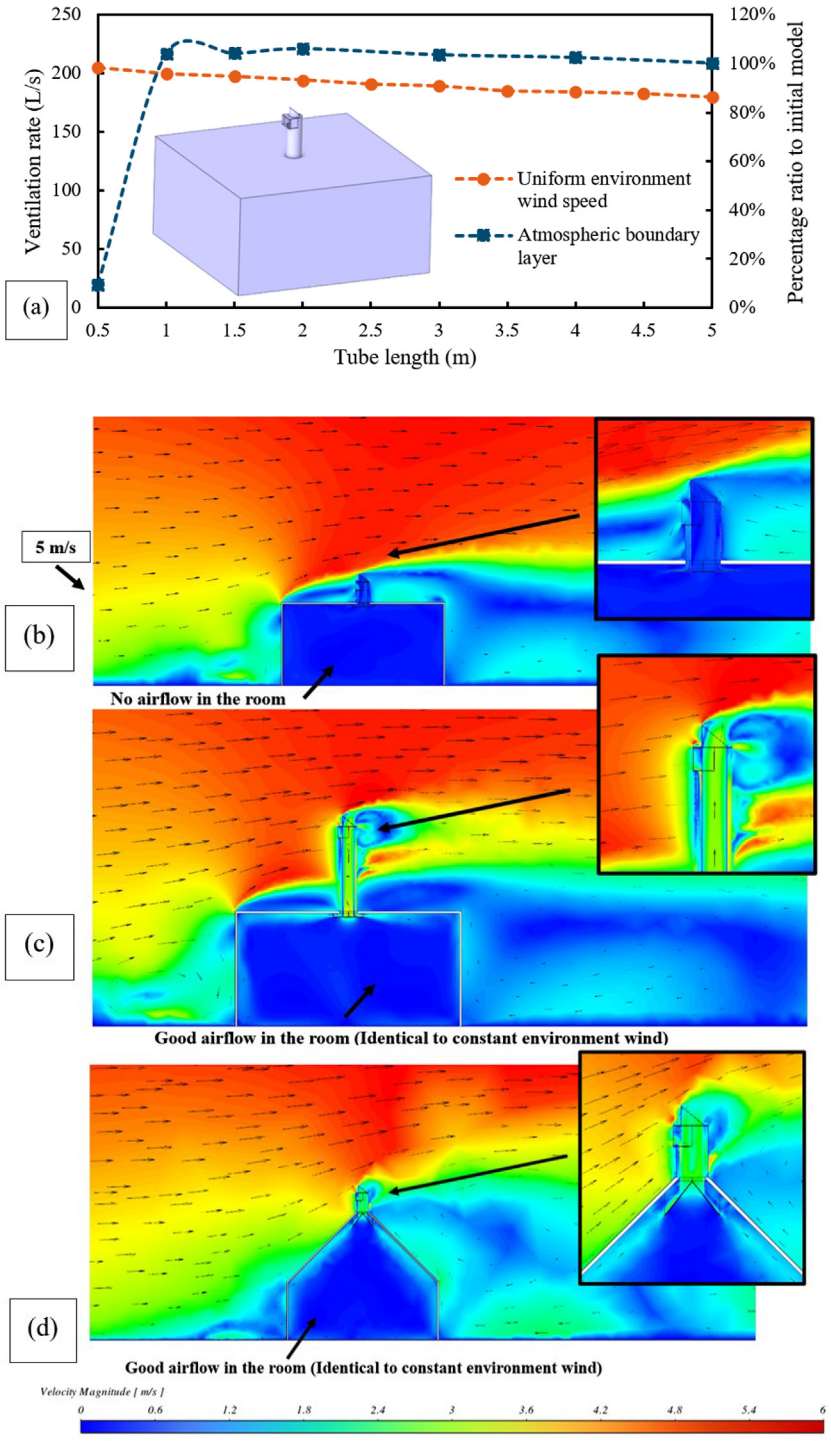

Fig. 16. (a) Impact of the windcatcher height on the ventilation rate at 5 m/s uniform outdoor wind speed and full-scale simulation with atmospheric boundary layer. Cross-sectional contour of the velocity for the full-scale simulation of windcatcher with (b) initial height, (c) adjusted height (2 m), and (d) initial height with pitched roof building.

Table 2
Parametric analysis summary

Parametric analysis	Initial value	Parameter range	Optimized value	Ventilation rate (L/s)	Ventilation rate improvement
Internal diameter	300 mm	0–450 mm	320 mm	161.6	1.0 %
Wing wall	Not applied	0–90° 50–200 mm	20° 50 mm	170.6	6.6 %
Wind scoop opening height	200 mm	0–500 mm	300 mm	179.2	12.0 %
Chamfered chimney	Not applied	0–60°	40°	181.2	13.2 %
ASCD height	100 mm	0–200 mm	100 mm	160	0 %
Final model					28.0 %

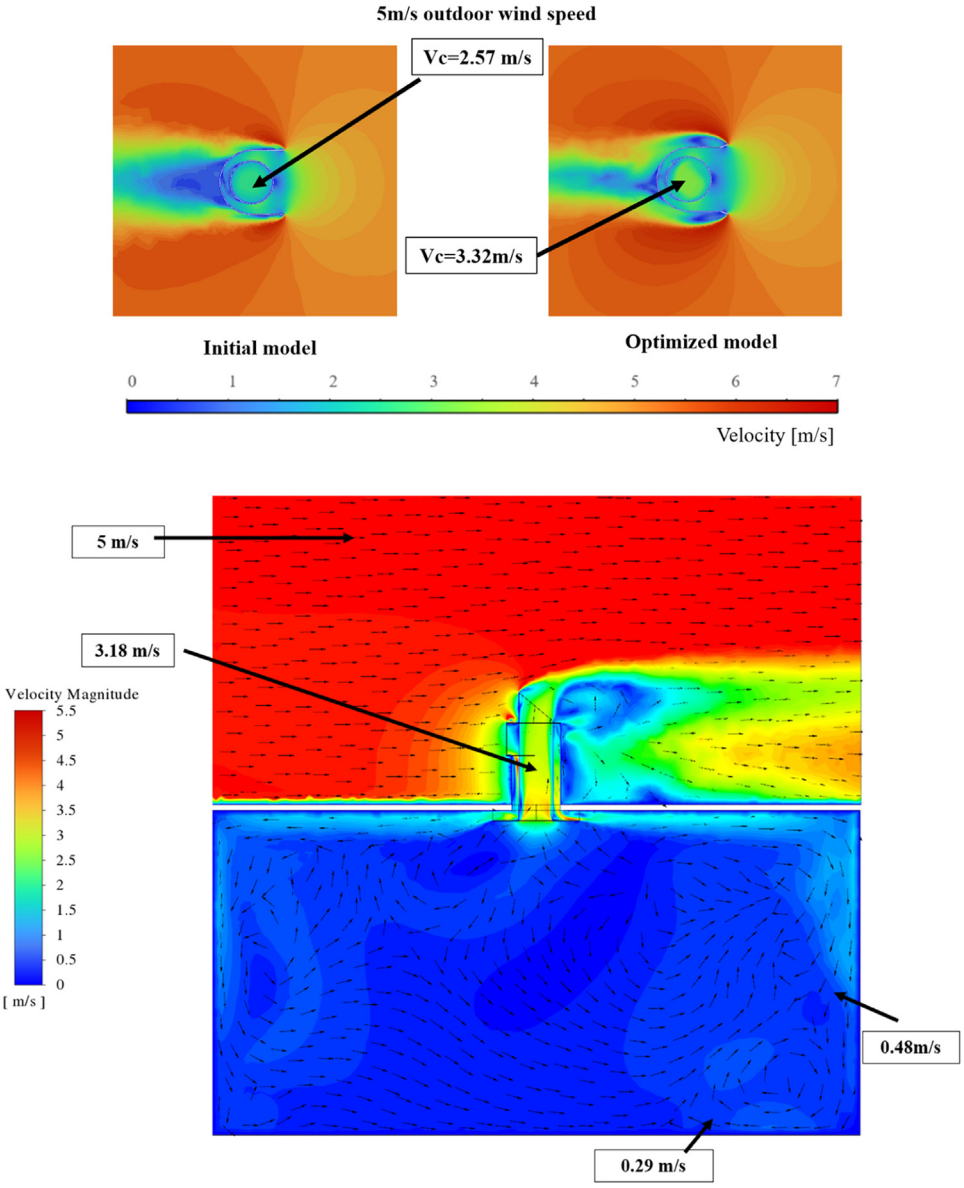

Fig. 17. Velocity contours and vectors showing the airflow distribution in the modified rotary scoop windcatcher at 5 m/s outdoor wind speed, and a comparison of the airflow distribution in the initial and optimized model at the wind scoop region..

chimney provided the most significant single improvement of 13.2 %, followed closely by the wind scoop opening height at 12 %. The wing wall and internal diameter adjustments also contributed to the performance enhancement but to a lesser extent compared to the chimney and wind scoop modifications. The final iteration of the optimized model presented a combination of modifications, incorporating a chamfered angle of 40°, a wind scoop height of 300 mm, an internal-to-external diameter ratio of 320 mm to 450 mm, and a 50 mm wing wall set at a 20-degree installation angle as presented in Table 2. The initial ASCD height was applied as the increase in the ASCD gap did not increase the ventilation rate of the windcatcher.

To evaluate the performance of the optimized windcatcher, simulations were conducted under constant environmental wind speed conditions of 5 m/s. The velocity distribution within the windcatcher system was analyzed and visualized through velocity contours, as shown in Fig. 17. It was observed that the airflow within the room maintained effective circulation, ensuring the supply of fresh air to the lower levels at a comfortable velocity while facilitating efficient extraction after circulation.

Moreover, the pressure distribution within the windcatcher system was analyzed and presented through pressure contours, as depicted in Fig. 18. Comparing the optimized windcatcher to its initial design, noticeable changes in the pressure differentials were observed. The positive pressure at the inlet experienced a slight increase from 11.4 Pa to 12.6 Pa, while the negative pressure at the outlet exhibited a significant increase from −0.7 Pa to −5.2 Pa. This substantial increase in negative pressure resulted in a rise in the pressure differential between the inlet and outlet, escalating by 47 % from 12.1 Pa to 17.8 Pa. These findings demonstrate the improved performance of the windcatcher system in generating a stronger pressure differential, which facilitates enhanced airflow and ventilation efficiency under 5 m/s environmental wind speed conditions.

3.8. Comparison with a conventional two-sided and four-sided windcatcher

To provide a comprehensive comparative analysis, the conventional four-sided windcatcher was included alongside the optimized and initial rotary scoop windcatchers. Fig. 19 (a) presents the ventilation performance of these windcatcher designs, revealing notable differences in their capabilities. The optimized windcatcher exhibited an enhancement in overall ventilation rate, surpassing the initial model by 28 %. Furthermore, when compared to the four-sided windcatcher of the same di-

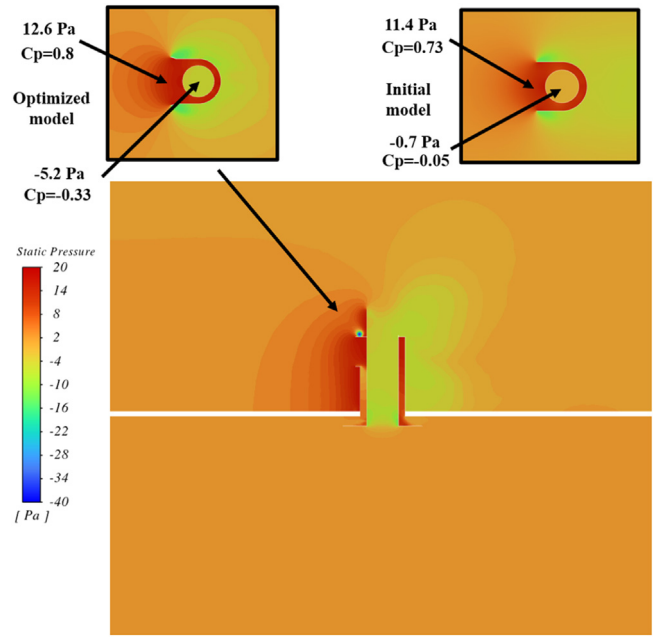

Fig. 18. Pressure contour showing the pressure distribution in the optimized rotary scoop windcatcher at 5 m/s outdoor wind speed, and a comparison of the pressure distribution in the initial and optimized model at the wind scoop region.

mensions and under identical environmental wind speed conditions, the modified windcatcher demonstrated an improvement in ventilation performance. Specifically, the ventilation rates achieved by the optimized windcatcher ranged from 14 % to 58 % higher than those of the four-sided windcatcher. Moreover, the ventilation performance of the rotary windcatcher is higher than that of the traditional two-side windcatcher with the same section area, as observed in Fig. 19. The modified windcatcher not only delivered enhanced ventilation rates given the same area but also ensured a stable supply of fresh air, which remained unaffected by fluctuating wind directions in the surrounding environment.

4. Discussion of study limitations and practical considerations

In the present design of the windcatcher under consideration, an open chimney structure has been employed. The primary rationale behind adopting such a straightforward construction was to simplify this investigation, with the core objective being the examination of multi-directional natural ventilation facilitated through the innovative rotary scoop design. The focus, therefore, was on exploring and optimizing the effects of the geometric parameters of the windcatcher on ventilation performance. However, it is crucial to scrutinize the practical implications of employing an open chimney in real-world applications. The feasibility of such a configuration, without any protective measures, may raise concerns, given the array of potential environmental elements it could be exposed to. Key elements of potential threat include weather-based factors like rainfall, along with small animals and insects, all of which could interfere with the operation of the windcatcher and even lead to detrimental effects on indoor air quality. Given these potential vulnerabilities, it becomes clear that the incorporation of protective

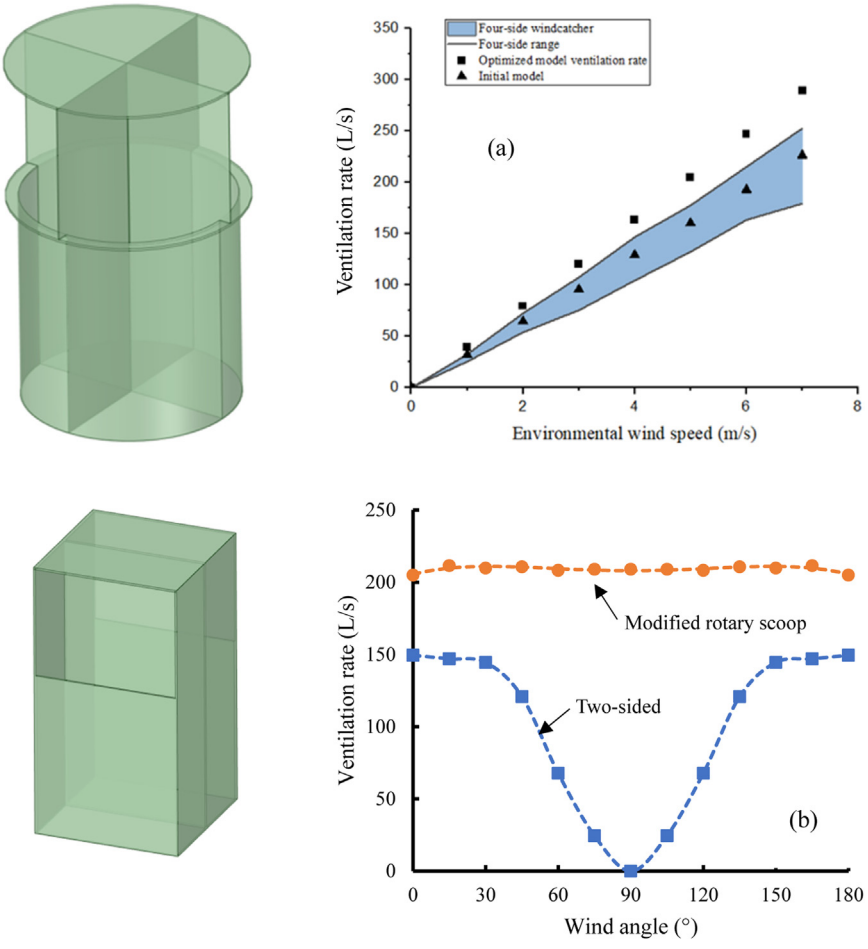

Fig. 19. (a) Comparison of the ventilation rates of the modified and initial rotary scoop windcatcher and the four-sided windcatcher, and (b) comparison of the ventilation rates of the two-side square windcatcher and modified rotary scoop windcatcher at different wind angles.

measures such as a chimney cap or cowl is a practical necessity. Such additions can effectively shield the outlet from various environmental elements, thereby maintaining the functional integrity of the windcatcher. Future design iterations should thus focus not only on optimization for ventilation performance but also on ensuring robustness against external environmental factors. This will help to ensure that the windcatcher can operate effectively and consistently in a broad range of real-world conditions.

Furthermore, the current design of the windcatcher involves a bearing system that connects the rotary wind scoop to the tubes. It is observed that this bearing configuration does not provide a perfect seal between the rotating wind scoop and the static tubes, allowing for a potential gap. While this may seem like a minor oversight in design, it is of importance to minimize this gap, as it can provide a pathway for a possible short circuit from the inlet to the outlet. Such a short circuit would essentially bypass the intended airflow path, thereby undermining the windcatcher's ventilation performance. One potential solution to address this issue might involve the use of a ring-shaped bearing. This configuration could potentially seal off the identified gap. However, the implications of adopting such a solution must be carefully examined. The introduction of a ring-shaped bearing would likely result in increased friction, necessitating the inclusion of a larger tailplane. This, in turn, could significantly elevate both the initial capital investment and the ongoing maintenance costs relative to the current bearing system. Moreover, it would inherently increase the frictional forces, thus raising the torque requirements for rotating the wind scoop. This could introduce further complexities to the design and operational aspects of the windcatcher.

Considering these factors, the current bearing design appears to be more advantageous for the device. Its low maintenance demand and overall reliability appear to outweigh the potential benefits of the previously considered ring-shaped bearing. In this context, it is essential to prioritize system stability and reliability, even at the expense of some potential efficiency in ventilation performance. As such, while it remains important to strive for optimal ventilation efficiency, these other factors must also be considered in the design and implementation of the windcatcher system.

The proposed windcatcher and tube system can be manufactured from a selection of diverse materials to serve varying purposes. Transparent acrylic materials, for example, are an appealing choice as they allow daylight to filter through, providing natural lighting for the interior space. On the other hand, the choice of metal materials could serve to enhance the system's structural strength, durability, and cost-effectiveness. A particularly intriguing application could be to construct the external duct from transparent material while coating the internal duct in black. This combination creates a fascinating interplay of solar radiation absorption and heat emission. The internal duct, being black, would efficiently absorb solar radiation, converting it into heat. The heat, in turn, is emitted to both the supply and return air. This process can serve to preheat the supply air in the outside channel and create a solar chimney in the inside channel. The system can be further refined to incorporate passive or low-energy cooling into the supply channel. Such a mechanism can precool the supply air, particularly under suitable weather conditions. This feature can enhance thermal comfort within the indoor environment, and also reduce the consumption of cooling energy, thus contributing to the overall energy efficiency of the system.

In light of prior research [44], passive heat recovery techniques, such as the use of heat pipes or fins can also be integrated into the windcatcher channels. Given that the supply and return channels are in constant proximity and their airflow directions remain fixed regardless of wind direction, these heat recovery techniques could significantly enhance system efficiency.

It should be noted that in this study, the process of determining the dimensions of the windcatcher for experimental validation had to take into account several key factors. This included the dimensions of the blower-fan open wind tunnel available for the experimental process, and the constraints imposed by the available spatial limits. Additional constraints, such as the need to achieve uniform wind conditions and the necessity to reach specific wind velocities, further necessitated a limit on the size of the windcatcher under examination. The overarching goal of this investigation was to validate the computational model through the use of experimental measurements. To achieve this, it was of paramount importance that the geometric properties of the windcatcher be identically replicated in the numerical modelling efforts. Moreover, any subsequent optimization processes needed to be performed on the basis of this validated geometry. This methodological approach provided the foundation for a fair and objective comparison between the experimental and CFD investigations. In real-world applications, the determination of the windcatcher's dimensions would be governed by different factors. This might include considering the area or volume of the building in which the windcatcher will be installed and the specific ventilation requirements associated with the building, as underscored by prior research [71,72].

Furthermore, the cross-sectional area of the blower fan open wind tunnel was larger than the windcatcher model in the experiment to provide sufficient airflow but the blower fan was unable to provide uniform free-flowing airflow which is much larger than the windcatcher identical to the real environment. Thus, full-scale simulations of the windcatcher with ABL and uniform wind profiles were simulated after validating the experiment model. Further research should consider investigating the ventilation performance of a full-scale windcatcher in a larger wind tunnel with a uniform wind speed profile and the field test in the real environment. This would entail conducting field tests or utilizing larger wind tunnels to assess the windcatcher's functionality. Additionally, comparative studies examining windcatchers of various sizes and their ventilation rates, when installed in different buildings, would further contribute to the body of knowledge surrounding this innovative ventilation technology.

5. Conclusion and future works

In this research, a numerical technique using CFD simulation was developed based on an experimentally validated windcatcher model. The parametric CFD analysis of a multi-directional dual-channel rotary scoop windcatcher was conducted, modifying the windcatcher geometry to deliver enhanced ventilation efficiency compared to the existing systems. The windcatcher system offered several advantages over the fixed windcatcher, including (1) consistency in the position and airflow directions of the supply and return channels regardless of changes in environmental wind directions; (2) high ventilation efficiency unaffected by variable wind directions; and (3) potential for incorporating passive or low-energy heating, cooling, and heat recovery within the windcatcher's natural ventilation system. The process involved a detailed investigation of numerous parameters within the validated CFD model of the rotary scoop windcatcher. These parameters encompassed: (1) the ratio of the area of the supply channel to that of the return channel; (2) the angle and length of the wing walls; (3) the height of the wind scoop; (4) the angles of the chamfered chimneys; (5) the height of the ASCD; and (6) the height of the windcatcher tube. In order to fully assess the windcatcher's performance, a full-scale simulation of the device with various heights was undertaken. Moreover, the performance of the windcatcher installed above a pitched roof building was also studied to better understand the influence of wind speed traversing the roof on the windcatcher's ventilation performance.

The modified windcatcher model showed a 28 % increase in the overall ventilation rate compared to the initial model. Furthermore, its ventilation performance surpassed that of a four-sided windcatcher of equivalent size, with improvements ranging from 4 % to 58 % higher, under identical environmental wind speed conditions. This highlights the effectiveness of the optimization strategies in enhancing the windcatcher's ability to capture and circulate fresh air. Additionally, the pressure differential between the windcatcher's inlet and outlet experienced

a substantial 47 % increase at an outdoor wind speed of 5 m/s. This increase in pressure difference indicates the improved airflow dynamics and ventilation efficiency achieved by the modified windcatcher design.

In future research, it is crucial to explore the integration of passive or low-energy heating, cooling, and energy recovery technologies within the windcatcher system. Investigating the feasibility and performance of passive heating techniques utilizing solar thermal energy, as well as exploring passive cooling methods such as evaporative cooling, would provide valuable insights for achieving a more comprehensive and sustainable natural ventilation system. Furthermore, evaluating potential passive dehumidification approaches would contribute to enhancing indoor air quality and thermal comfort. To expand the knowledge base in this field, it is recommended to conduct experimental studies and field investigations to validate and refine the findings of this research. Experimental testing in a larger wind tunnel environment would allow for the assessment of windcatchers of varying sizes and configurations, providing a more comprehensive understanding of their ventilation performance under different conditions. Field studies in buildings would further validate the effectiveness of the windcatcher design and explore its practical application in diverse architectural and engineering contexts. The technology described here is patented with the reference number ZL 202320144680.9.

Declaration of competing interest

The authors declare that they have no known competing financial interests or personal relationships that could have appeared to influence the work reported in this paper.

CRediT authorship contribution statement

Jiaxiang Li: Writing – review & editing, Writing – original draft, Visualization, Validation, Software, Resources, Project administration, Methodology, Investigation, Formal analysis, Data curation, Conceptualization. **John Calautit:** Writing – review & editing, Supervision, Project administration, Conceptualization. **Carlos Jimenez-Bescos:** Supervision, Project administration.

Supplementary materials

Supplementary material associated with this article can be found, in the online version, at doi:10.1016/j.enbenv.2024.07.002.

Appendix

Wind speed function in the CFD model validation (r is distance to the centre of the wind blower outlet).

Average wind speed (m/s)	Wind speed profile function (m/s)
2.31	$v = -48.2 \times r^2 + 7.7 \times r + 2.33$
2.10	$v = -42.8 \times r^2 + 6.3 \times r + 2.27$
1.90	$v = -16.4 \times r^2 + 2.2 \times r + 1.98$
1.68	$v = -27.2 \times r^2 + 3.8 \times r + 1.79$
1.40	$v = -17.4 \times r^2 + 1.7 \times r + 1.53$
1.03	$v = -14.1 \times r^2 + 1.8 \times r + 1.07$
0.79	$v = -8.2 \times r^2 + 1.2 \times r + 0.81$
0.48	$v = -6.5 \times r^2 + 0.9 \times r + 0.49$

References

[1] O. Saadatian, L.C. Haw, K. Sopian, M.Y. Sulaiman, Review of windcatcher technologies, Renew. Sustain. Energy Rev. 16 (3) (2012) 1477–1495.
[2] B.J. He, L. Yang, M. Ye, B. Mou, Y. Zhou, Overview of rural building energy efficiency in China, Energy Pol. 69 (2014) 385–396.
[3] C.J. Rhodes, The 2015 Paris Climate Change Conference: cop21, Sci. Prog. 99 (1) (2016) 97–104.
[4] F. Jomehzadeh, H.M. Hussen, J.K. Calautit, P. Nejat, M.S. Ferwati, Natural ventilation by windcatcher (Badgir): a review on the impacts of geometry, microclimate and macroclimate, Energy Build.. 226 (2020) 110396.
[5] N.Z. Ghalam, M. Farrokhzad, H. Nazif, Investigation of optimal natural ventilation in residential complexes design for temperate and humid climates, Sustain. Energy Grid. Netw. 27 (2021) 100500.
[6] M. Fan, Z. Fu, J. Wang, Z. Wang, H. Suo, X. Kong, H. Li, A review of different ventilation modes on thermal comfort, air quality and virus spread control, Build. Environ. 212 (2022) 108831.
[7] K. Chen, Q. Xu, B. Leow, A. Ghahramani, Personal thermal comfort models based on physiological measurements – A design of experiments based review, Build. Environ. 228 (2023) 109919.
[8] Y. Xie, Z. Ding, J. Ma, X. Zheng, F. Liu, Y. Ding, Z. Shu, H. Qian, The assessment of personal exposure in restaurants considering heat sources and ventilation strategies, Energy Built Environ. 5 (5) (2024) 657–664.
[9] H. Yin, Z. Li, X. Zhai, Y. Ning, L. Gao, H. Cui, Z. Ma, A. Li, Field measurement of the impact of natural ventilation and portable air cleaners on indoor air quality in three occupant states, Energy Built Environ. 4 (5) (2023) 601–613.
[10] L. Pérez-Lombard, J. Ortiz, C. Pout, A review on buildings energy consumption information, Energy Build.. 40 (3) (2008) 394–398.
[11] H.-Y. Chan, S.B. Riffat, J. Zhu, Review of passive solar heating and cooling technologies, Renew. Sustain. Energy Rev. 14 (2) (2010) 781–789.
[12] J. Li, C. Jimenez-Bescos, J.K. Calautit, J. Yao, Evaluating the energy-saving potential of earth-air heat exchanger (EAHX) for Passivhaus standard buildings in different climates in China, Energy Build.. (2023) 113005.
[13] K. Pelletier, J. Calautit, Analysis of the performance of an integrated multistage helical coil heat transfer device and passive cooling windcatcher for buildings in hot climates, J. Build. Eng. 48 (2022) 103899.
[14] P.K. Sangdeh, N. Nasrollahi, Windcatchers and their applications in contemporary architecture, Energy Built Environ. 3 (1) (2022) 56–72.
[15] Y. He, Y. Chu, H. Zang, J. Zhao, Y. Song, Experimental and CFD study of ventilation performance enhanced by roof window and mechanical ventilation system with different design strategies, Build. Environ. 224 (2022) 109566.
[16] C.E. Vázquez-Torres, A. Gómez-Amador, Impact of indoor air volume on thermal performance in social housing with mixed mode ventilation in three different climates, Energy Built Environ. 3 (4) (2022) 433–443.
[17] E. Bay Sahin, A. Martinez-Molina, W. Dupont, Assessment of natural ventilation strategies in historical buildings in a hot and humid climate using energy and CFD simulations, J. Build. Eng. 51 (2022) 104287.
[18] H. Zhang, D. Yang, V.W.Y. Tam, Y. Tao, G. Zhang, S. Setunge, L. Shi, A critical review of combined natural ventilation techniques in sustainable buildings, Renew. Sustain. Energy Rev. 141 (2021) 110795.
[19] K. Bamdad, S. Matour, N. Izadyar, T. Law, SIntroducing extended natural ventilation index for buildings under the present and future changing climates, Build. Environ. (2022) 109688.
[20] S. Jafari, V. Kalantar, Numerical simulation of natural ventilation with passive cooling by diagonal solar chimneys and windcatcher and water spray system in a hot and dry climate, Energy Build. 256 (2022) 111714.
[21] M. Ghoulem, K. El Moueddeb, E. Nehdi, F. Zhong, J. Calautit, Analysis of passive downdraught evaporative cooling windcatcher for greenhouses in hot climatic conditions: parametric study and impact of neighbouring structures, Biosyst. Eng. 197 (2020) 105–121.
[22] A. Noroozi, Y. Veneris, Thermal Assessment of a Novel Combine Evaporative Cooling Wind Catcher, Energies 11 (2018) 442.
[23] J.K. Calautit, B.R. Hughes, S.S. Shahzad, CFD and wind tunnel study of the performance of a uni-directional wind catcher with heat transfer devices, Renew. Energy 83 (2015) 85–99.
[24] Z.M. Gilvaei, A.H. Poshtiri, A.M. Akbarpoor, A novel passive system for providing natural ventilation and passive cooling: evaluating thermal comfort and building energy, Renew. Energy (2022).
[25] H. Montazeri, R. Azizian, Experimental study on natural ventilation performance of a two-sided wind catcher, Proceed. Instit. Mech. Eng., Part A: J. Power Energy 223 (4) (2009) 387–400.
[26] H. Montazeri, R. Azizian, Experimental study on natural ventilation performance of one-sided wind catcher, Build. Environ. 43 (12) (2008) 2193–2202.
[27] S. MRKhani, M.N. Bahadori, A.R. Dehghani-Sanij, Experimental investigation of a modular wind tower in hot and dry regions, Energy Sustain. Develop. 39 (2017) 21–28.
[28] S. Liu, C.M. Mak, J. Niu, Numerical evaluation of louver configuration and ventilation strategies for the windcatcher system, Build. Environ. 46 (8) (2011) 1600–1616.
[29] Z. Moghtader Gilvaei, A.H. Poshtiri, A. Mirzazade Akbarpoor, A novel passive system for providing natural ventilation and passive cooling: evaluating thermal comfort and building energy, Renew. Energy 198 (2022) 463–483.
[30] J. Foroozesh, S.H. Hosseini, A.J. Ahmadian Hosseini, F. Parvaz, K. Elsayed, N. Uygur Babaoğlu, K. Hooman, G. Ahmadi, CFD modeling of the building integrated with a novel design of a one-sided wind-catcher with water spray: focus on thermal comfort, Sustain. Energy Technolog. Assessm. 53 (2022) 102736.
[31] M. Afshin, A. Sohankar, M.D. Manshadi, M.K. Esfeh, An experimental study on the evaluation of natural ventilation performance of a two-sided wind-catcher for various wind angles, Renew. Energy 85 (2016) 1068–1078.
[32] L. Moosavi, M. Zandi, M. Bidi, E. Behroozizade, I. Kazemi, New design for solar chimney with integrated windcatcher for space cooling and ventilation, Build. Environ. 181 (2020) 106785.
[33] B. Zhang, C.Y. Li, H. Kikumoto, J. Niu, T.K.T. Tse, Smart urban windcatcher: conception of an AI-empowered wind-channeling system for real-time enhancement of urban wind environment, Build. Environ. 253 (2024) 111357.
[34] M. Liu, S. Almazmumi, P. Cao, C. Jimenez-bescos, J.K. Calautit, Can windcatcher's natural ventilation beat the chill? A view from heat loss and thermal discomfort, Build. Environ. 247 (2024) 110916.

[35] L. Li, C.M. Mak, The assessment of the performance of a windcatcher system using computational fluid dynamics, Build. Environ. 42 (3) (2007) 1135–1141.
[36] B.M. Jones, R. Kirby, Quantifying the performance of a top–down natural ventilation Windcatcher™, Build. Environ. 44 (9) (2009) 1925–1934.
[37] M. Liu, C. Jimenez-Bescos, J. Calautit, CFD investigation of a natural ventilation wind tower system with solid tube banks heat recovery for mild-cold climate, J. Build. Eng. 45 (2022) 103570.
[38] J.K. Calautit, D. O'Connor, B.R. Hughes, A natural ventilation wind tower with heat pipe heat recovery for cold climates, Renew. Energy 87 (2016) 1088–1104.
[39] H. Mahon, D. Friedrich, B. Hughes, Wind tunnel test and numerical study of a multi-sided wind tower with horizontal heat pipes, Energy 260 (2022) 125118.
[40] J.K. Calautit, D. O'Connor, P.W. Tien, S. Wei, C.A.J. Pantua, B. Hughes, Development of a natural ventilation windcatcher with passive heat recovery wheel for mild-cold climates: CFD and experimental analysis, Renew. Energy 160 (2020) 465–482.
[41] C.A. Varela-Boydo, S.L. Moya, R. Watkins, Analysis of traditional windcatchers and the effects produced by changing the size, shape, and position of the outlet opening, J. Build. Eng. 33 (2021) 101828.
[42] H. Montazeri, F. Montazeri, R. Azizian, S. Mostafavi, Two-sided wind catcher performance evaluation using experimental, numerical and analytical modeling, Renew. Energy 35 (7) (2010) 1424–1435.
[43] M. Farouk, Comparative study of hexagon & square windcatchers using CFD simulations, J. Build. Eng. 31 (2020) 101366.
[44] J. Li, J. Calautit, C. Jimenez-Bescos, S. Riffat, Experimental and numerical evaluation of a novel dual-channel windcatcher with a rotary scoop for energy-saving technology integration, Build. Environ. (2023) 110018.
[45] P.V. Dorizas, S. Samuel, M. Dejan, Y. Keqin, M.-M. Dimitris, L. Tom, Performance of a natural ventilation system with heat recovery in UK classrooms: an experimental study, Energy Build. 179 (2018) 278–291.
[46] Y. Jiang, Q. Chen, Effect of fluctuating wind direction on cross natural ventilation in buildings from large eddy simulation, Build. Environ. 37 (4) (2002) 379–386.
[47] N. Khan, Y. Su, S.B. Riffat, A review on wind driven ventilation techniques, Energy Build. 40 (8) (2008) 1586–1604.
[48] J. Li, J.K. Calautit, C. Jimenez-Bescos, Experiment and numerical investigation of a novel flap fin louver windcatcher for multi-directional natural ventilation and passive technology integration, Build. Environ. 242 (2023) 110429.
[49] N. Kumar, R. Bardhan, T. Kubota, Y. Tominaga, M. Shirzadi, Parametric study on vertical void configurations for improving ventilation performance in the mid-rise apartment building, Build. Environ. 215 (2022) 108969.
[50] M. Liu, P. Nejat, P. Cao, C. Jimenez-Bescos, J.K. Calautit, A critical review of windcatcher ventilation: micro-environment, techno-economics, and commercialisation, Renew. Sustain. Energy Rev. 191 (2024) 114048.
[51] S. Heidari, A.H. Poshtiri, Z.M. Gilvaei, Enhancing thermal comfort and natural ventilation in residential buildings: a design and assessment of an integrated system with horizontal windcatcher and evaporative cooling channels, Energy 289 (2024) 130040.
[52] P. Nejat, M. Salim Ferwati, J. Calautit, A. Ghahramani, M. Sheikhshahrokhdehkordi, Passive cooling and natural ventilation by the windcatcher (Badgir): an experimental and simulation study of indoor air quality, thermal comfort and passive cooling power, J. Build. Eng. 41 (2021) 102436.
[53] M. Ghoulem, K. El Moueddeb, E. Nehdi, F. Zhong, J.K. Calautit, Design of a passive downdraught evaporative cooling windcatcher (PDEC-WC) system for greenhouses in hot climates, Energies 13 (2020) 2934.
[54] M. Khakzand, B. Deljouiee, S. Chahardoli, M. Siavashi, Radiative cooling ventilation improvement using an integrated system of windcatcher and solar chimney, J. Build. Eng. 83 (2024) 108409.
[55] J.P. Harrouz, K. Ghali, N. Ghaddar, Integrated solar – windcatcher with dew-point indirect evaporative cooler for classrooms, Appl. Therm. Eng. 188 (2021) 116654.
[56] J. Li, J. Calautit, C. Jimenez-Bescos, S. Riffat, Experimental and numerical evaluation of a novel dual-channel windcatcher with a rotary scoop for energy-saving technology integration, Build. Environ. 230 (2023) 110018.
[57] P. Nejat, J.K. Calautit, M.Z.A. Majid, B.R. Hughes, F. Jomehzadeh, Anti-short-circuit device: a new solution for short-circuiting in windcatcher and improvement of natural ventilation performance, Build. Environ. 105 (2016) 24–39.
[58] J.H. Bell, R.D. Mehta, Design and Calibration of the Mixing Layer and Wind Tunnel, 1989.
[59] S.H. Hosseini, E. Shokry, A.J. Ahmadian Hosseini, G. Ahmadi, J.K. Calautit, Evaluation of airflow and thermal comfort in buildings ventilated with wind catchers: simulation of conditions in Yazd City, Iran, Energy Sustain. Develop. 35 (2016) 7–24.
[60] T. Kobayashi, M. Sandberg, T. Fujita, E. Lim, N. Umemiya, Numerical analysis of wind-induced natural ventilation for an isolated cubic room with two openings under small mean wind pressure difference, Build. Environ. (2022) 109694.
[61] B.R. Hughes, J.K. Calautit, S.A. Ghani, The development of commercial wind towers for natural ventilation: a review, Appl. Energy 92 (2012) 606–627.
[62] M. Ghadiri, M. Dehnavi, The Effect of Plan Size in Wind Catcher on its Ventilation Rate, 2014.
[63] V. Zmrhal, J. Boháč, Pressure loss of flexible ventilation ducts for residential ventilation: absolute roughness and compression effect, J. Build. Eng. 44 (2021) 103320.
[64] C.F. Colebrook, C.M. White, G.I. Taylor, Experiments with fluid friction in roughened pipes, Proceed. Roy. Soc. Lond. Ser. A - Math. Phys. Sci. 161 (906) (1937) 367–381.
[65] Y. Taitel, A.E. Dukler, A model for predicting flow regime transitions in horizontal and near horizontal gas-liquid flow, AIChE J. 22 (1) (1976) 47–55.
[66] C.M. Mak, J.L. Niu, C.T. Lee, K.F. Chan, A numerical simulation of wing walls using computational fluid dynamics, Energy Build. 39 (9) (2007) 995–1002.
[67] P. Nejat, J.K. Calautit, M.Z.A. Majid, B.R. Hughes, I. Zeynali, F. Jomehzadeh, Evaluation of a two-sided windcatcher integrated with wing wall (as a new design) and comparison with a conventional windcatcher, Energy Build. 126 (2016) 287–300.
[68] A.A. Elmualim, H.B. Awbi, Wind Tunnel and CFD Investigation of the Performance of "Windcatcher" Ventilation Systems, Int. J. Ventilat. 1 (1) (2002) 53–64.
[69] M.K. Esfeh, A. Sohankar, A.R. Shahsavari, M.R. Rastan, M. Ghodrat, M. Nili, Experimental and numerical evaluation of wind-driven natural ventilation of a curved roof for various wind angles, Build. Environ. 205 (2021) 108275.
[70] M.N. Bahadori, F. Haghighat, Passive cooling in hot, arid regions in developing countries by employing domed roofs and reducing the temperature of internal surfaces, Build. Environ. 20 (2) (1985) 103–113.
[71] J.K. Calautit, B.R. Hughes, D. O'Connor, S.S. Shahzad, Numerical and experimental analysis of a multi-directional wind tower integrated with vertically-arranged heat transfer devices (VHTD), Appl. Energy 185 (2017) 1120–1135.
[72] P. Nejat, J.K. Calautit, Y. Fekri, M. Sheikhshahrokhdehkordi, H. Alsaad, C. Voelker, Influence of terrain and atmospheric boundary layer on the ventilation and thermal comfort performance of windcatchers, J. Build. Eng. 73 (2023) 106791.